Climate Change Ecology 3 (2022) 100049

Contents lists available at ScienceDirect

Climate Change Ecology

journal homepage: www.elsevier.com/locate/ecochg

High-latitude calcified coralline algae exhibit seasonal vulnerability to acidification despite physical proximity to a non-calcified alga

LE Bell[a,*], JB Gómez[a], E Donham[a], DL Steller[b], PW Gabrielson[c], KJ Kroeker[a]

[a] Ecology and Evolutionary Biology, University of California Santa Cruz, 130 McAllister Way, Santa Cruz, CA 95060, United States of America
[b] Moss Landing Marine Laboratories, 8272 Moss Landing Rd, Moss Landing, CA 95039, United States of America
[c] Herbarium and Department of Biology, University of North Carolina, Chapel Hill, NC 27599, United States of America

ARTICLE INFO

Keywords:
Ocean acidification (OA)
Global change
Calcification
Interaction
Bossiella
Crusticorallina

ABSTRACT

The emergent responses of vulnerable species to global change can vary depending on the relative quality of resources available to support their productivity under increased stress, as well as the biotic interactions with other species that may alter their access to these resources. This research tested how seawater pCO_2 may interact with seasonal light availability to affect the photosynthesis and calcification of high-latitude coralline algae, and whether the responses of these calcified macroalgae are modified by physical association with a non-calcified seaweed. Through an in situ approach, our study first investigated how current seasonal environmental variation affects the growth of the understory coralline algae *Crusticorallina* spp. and *Bossiella orbigniana* in Southeast Alaska's kelp forests. We then experimentally manipulated pH to simulate end-of-century acidification scenarios, light regime to simulate seasonal light availability at the benthos, and pairings of coralline algal species with and without a fleshy red alga to examine the interactive effects of these variables on coralline productivity and calcification. Our results indicate that: 1) coralline species may face net dissolution under projected future winter pH and carbonate saturation state conditions, 2) differences in seasonal light availability in productive, high-latitude waters may not be distinct enough to modify coralline algal net calcification, and 3) association with a non-calcified red alga does not alter the response of these coralline algal species to ocean acidification scenarios. This research highlights the necessity of incorporating locally informed scenarios of environmental variability and community interactions when predicting species' vulnerability to global change.

1. Introduction

The emergent effects of global change on the ecology of individual species will ultimately depend on environment-ecosystem interactions. In particular, a given species' response will be shaped by the rate and magnitude of environmental change on the mean, variability, and extremes characteristic of their local environment. These regional attributes of an organism's environment are influenced both by large-scale physical forces, as well as smaller scale interactions with other species [e.g., 1–5]. Furthermore, temporal variability in environmental conditions is often multivariate, such that variability in one abiotic driver often covaries with other drivers that can mediate species' responses to change. Understanding the emergent effects of global change therefore requires careful attention to the local characteristics of the environment experienced by organisms in nature.

Ocean acidification (OA) is a global process that threatens marine species worldwide [6]. Most research considering marine species' responses to OA has been limited to short-term, static manipulations of carbonate chemistry in laboratory settings derived from mean environmental conditions. In nature, marine organisms experience pronounced temporal variability in carbonate chemistry, as well as other environmental factors that could mediate their response to OA [7,8]. For example, high-latitude regions illustrate how temporal variability in carbonate chemistry, primarily seasonal in nature, aligns with seasonal variability in other ecologically important conditions. Specifically, seawater pH and carbonate saturation states are lowest during winter months at high latitude [9–12], corresponding with the seasonal low in photoperiod. Marine macroalgae, which depend on carbon acquisition through photosynthesis, may be especially impacted by the potential interactions between OA and seasonal light availability characteristic of high latitudes [13–16]. Furthermore, macrophyte species widely considered vulnerable to OA are generally embedded in diverse communities, where their interactions with other species can modify their relative OA exposure and available light [17–20].

Calcium-carbonate containing coralline algae play an important ecological role in coastal marine ecosystems, often dominating benthic per-

* Corresponding author.
E-mail address: laebell@ucsc.edu (L. Bell).

https://doi.org/10.1016/j.ecochg.2022.100049
Received 1 June 2021; Received in revised form 27 December 2021; Accepted 1 January 2022
Available online 5 January 2022

cent cover on tropical to temperate rocky reefs [21,22]. Coralline algae provide structural habitat, food, and chemical settlement cues for a wide diversity of invertebrate larvae [23–26]. The high-magnesium calcite that these algae precipitate to form their thalli [27,28] is particularly vulnerable to dissolution under OA [29–31]. Reduced structural integrity, recruitment rate, and growth of coralline algae in high pCO_2 concentrations [32–35] could affect their ability to compete for space with non-calcified algae [36–40]. Given the foundational function of these reef-building calcifiers, future decreases in coralline algal abundance under OA may lead to myriad changes to coastal marine communities across the globe [41,42].

The ability of calcifying coralline algae to compensate for increased dissolution as OA progresses is dependent on available light, as calcification is linked to photosynthesis-driven carbonate chemistry changes at the thallus surface [43–45]. Sub-saturating irradiances exacerbate the effects of OA by reducing the available energy needed to offset increased respiration costs [16,46]. This dynamic is of particular interest at high latitudes, where seasonal variation in daylength and productivity already result in an overlapping winter window of decreased seawater pH and carbonate saturation state with reduced photoperiod that could be detrimental to marine calcifiers in the future [12]. Indeed, many species of temperate coralline algae exhibit their highest growth rates during the summer season when day lengths are longer, and temperature, pH, and saturation state are higher [47–50]. However, there are species of calcified algae that demonstrate resilience to OA exposure by maintaining high pH at their surface [51,52], and some Arctic coralline algae can maintain high surface pH and growth even under limited light or dark conditions by decoupling carbon fixation and reducing respiratory release of CO_2 [53,54]. While these examples suggest that some coralline algae may be resilient to future OA, no generalizable pattern based on habitat or evolutionary history has yet emerged to enable accurate predictions of the response of unstudied species [55].

Coralline algal physiology can be intimately tied to their interaction with canopies of closely associated non-calcifying macroalgae. The physical presence of canopy-forming algae, including turf and foliose forms of red and brown algae, can substantially attenuate water flow within a seaweed bed, as well as metabolically alter the seawater chemistry experienced by underlying calcifiers [19,20,56,57]. Macroalgae can modify carbonate chemistry in their associated boundary layers [53,58] and in surrounding habitats, as seen within the surface waters surrounding a *Macrocystis pyrifera* kelp forest canopy [59,60]. Such slow-flow boundary-layer habitats could facilitate growth and calcification of coralline algae in relatively acidic or undersaturated conditions [61–65], although the effect of reduced water velocity may be highly specific to species and habitat [66]. On the other hand, daytime benefits to coralline algae of increased pH and saturation state in the presence of a non-calcifying algal canopy can be offset by the relatively more acidic and less saturated environment experienced during nighttime respiration [20]. Enhanced diurnal pH fluctuations have been demonstrated to reduce growth rates and calcification of both juvenile and adult coralline algae, particularly in OA conditions [67–69]. Additionally, shading caused by neighboring algal canopies can directly impact photosynthesis, and the combination of low light and slower flow has been linked to reduced calcification for some coralline species [66,70]. In systems where coralline species are sensitive to changes in seawater carbonate chemistry, the specific interactions between macroalgal calcifiers and non-calcifiers may influence the direction of the aggregate response of coralline species to future OA.

The seaweed communities found along the outer coast of Southeast Alaska include the northernmost continuous band of *Macrocystis* kelp forests in the world, which also demarcate the northern and southern range limits of a suite of associated nearshore algal and invertebrate species [71]. Although this high-latitude crossover region of relatively high marine biodiversity is considered 'sub-polar', biological processes within the Gulf of Alaska are still governed by significant environmental seasonality, similar to that seen in higher Arctic waters. Heavy coastal precipitation in the fall and winter months combines with cold temperatures, short daylight hours, and reduced water column productivity to influence the carbonate chemistry of this system [10,11,72], leading to an annual pH minimum in late winter (Jan-Feb) [12]. This region is also susceptible to the rapid climatic changes already being observed at higher latitudes, where persistent undersaturation of marine surface waters is anticipated within the next 40 years [73,74]. The combination of biodiversity, seasonality and vulnerability to global change that characterizes the coastal seaweed communities of this area highlights their potential as bellwethers for how future increases in seawater pCO_2 may alter the responses and interactions among algal species in other, lower-latitude systems [75].

In this study, we explore how variation in carbonate chemistry and light availability impact the growth of high latitude coralline algae, and how their naturally close proximity to a non-calcified algal species may modulate these responses under future OA scenarios. To accomplish this, we incorporated both field monitoring and laboratory manipulation of species representing the two dominant coralline algal morphotypes in Southeast Alaska: erect, branched geniculate and crustose non-geniculate. Given the limited prior research on calcified coralline algae in this region and the necessity of using DNA sequencing to accurately distinguish morphologically ambiguous coralline algal species [76,77], we employed molecular methods to identify whether our findings applied to a species-specific or genus-specific level. By considering algal responses to OA in the context of their natural environmental variation as well as interactions with other species, this research answers a call to embrace ecological complexity to better understand community-level effects of global change [8,78,79].

2. Materials and methods

2.1. Subtidal light availability

Year-round variation in relative light intensity reaching the benthos on coralline reefs in Sitka Sound, AK was measured using submersible pendant light loggers (Onset HOBO). From 2017–2020, we intermittently deployed two light loggers at ~7 m depth (MLLW) at each of four rocky reef sites with high coralline algal cover and varied *Macrocystis pyrifera* kelp canopy cover (Harris Is.: 57.032 N, 135.277 W; Breast Is.: 57.039 N, 135.333 W; Samsing Pinnacle: 56.988 N, 135.357 W; Sandy Cove: 56.986 N, 135.321 W; Fig. A.1). At each site, both loggers were placed within 1 m of each other, oriented to face the water surface, and programmed to record light intensity (lux; lumen m^{-2}) every 30 min. We used two loggers at each site in order to correct for differences in orientation or macroalgal canopy cover immediately above the two loggers. The light loggers were cleaned every 1–3 mo, although overall fouling was low. To compare relative light availability at the benthos throughout the year, we transformed our data to integrate both daily variation in light intensity and seasonal variation in day length. For every day with a complete set of deployment data (both loggers recording for 24 h), we calculated the average total luminous exposure (lumen-hr m^{-2}) experienced at the benthos for each hour of the day and then summed these values to get an estimate of average luminous exposure at the benthos each calendar day of the year (lumens d^{-1} m^{-2}).

Because measurements of illumination (lux) do not necessarily correlate with the photosynthetic photon flux density (PPFD; μmol m^{-2} s^{-1}), which is more physiologically relevant to macroalgae, we also haphazardly recorded hundreds of instantaneous measurements of PPFD at the benthos in winter and summer seasons at each site using a Diving-PAM-II (Heinz Walz GmbH) MINI-SPEC. With these values, we generated average ranges of PPFD reaching the benthos, which were used to inform PPFD levels for the seasonal light regime treatments in the laboratory experiment (Section 2.4).

2.2. Coralline algae collection and species verification

We used DNA sequencing to identify the species represented by two spatially dominant morphotypes of crustose and geniculate coralline algae found subtidally in Sitka Sound. Individuals of each morphotype were collected from a subtidal rocky reef on Marshall Is., Sitka Sound, AK (57.032 N, 135.273 W) in Aug 2017. Crustose individuals targeted for collection were those that had a morphology that could easily be separated from the rocky substrate, often disk-shaped with distinct white growing edges. Geniculate individuals were collected to include the basal holdfast. The two morphotypes, which we initially grouped using morpho-anatomical cues, were the focus of our field (Section 2.3) and laboratory (Section 2.4) experiments. A subset of individuals of each morphotype that were used in the laboratory experiment (crustose: $n = 16$; geniculate: $n = 13$) were vouchered and desiccated in precipitated silica gel. Specimens were extracted following the protocol by Hughey et al. [80], as modified by Gabrielson et al. [81] for coralline algae. The primer pair F753/RrbcS [82] was used to amplify 694 bp of *rbc*L 3′ following Hughey et al. [80]. Contigs were assembled using Sequencher 5.2.4 (Gene Codes Corp., Ann Arbor, MI, USA), aligned in Geneious Prime (2020.2.4 Biomatters Ltd.) and subjected to BLAST analyses in GenBank.

The term *Crusticorallina* spp. was applied to the group of crustose individuals collected in the field and used in all experiments. Genetic analyses identified the group to contain 3 distinct species: *Crusticorallina painei, C. adhaerens, and C. muricata.* The physiological results apply to the group. The geniculate coralline species was verified as *Bossiella orbigniana*. All sequences were 100% matches to sequences of each of the taxa in GenBank, all of which have had their type specimens sequenced. Vouchers are deposited in NCU (Table A.1; herbarium acronym follows Index Herbariorum online [83]).

2.3. Seasonal growth rate of coralline algae

To assess *in-situ* seasonal changes in coralline algal growth rates, we collected specimens of *Crusticorallina* spp. and *B. orbigniana* in Dec 2017, July 2018, and Jan 2019 at Marshall Is., Sitka Sound. Individuals of each morphotype were cleaned by removing epiphytic algae and invertebrates with tweezers, and then placed in an aquarium of recirculating seawater with 100 mg L^{-1} concentration of the membrane-permeable live-cell labeling fluorescent dye Calcein for 6 h. This dye is absorbed by metabolically active meristematic tissue of the alga at the time of the stain [84], thus providing a growth benchmark for subsequently added tissue. After staining, each coralline individual (*Crusticorallina* spp.: a 'disc' with at least a 50% intact growing edge; *B. orbigniana*: a 'floret' containing 4–10 apical fronds) was attached to a small PVC stand by using z-spar epoxy putty to affix the older, non-meristematic tissue. Individuals on stands were then outplanted into the field on plates (2 crustose and 2 geniculate indiv. $plate^{-1}$) and bolted onto rocky reef substrate at 10 m depth MLLW at the edge of a giant kelp forest at Harris Is. Coralline algae were retrieved after 2–3mo, for total outplant durations of 67d (winter 2018), 66d (summer 2018), and 103d (winter 2019). Seawater pH and temperature during deployment periods were monitored with a SeapHOx sensor (Sea-Bird Scientific) [12] deployed within 10 m of the coralline outplant locations (mean ± SD: winter 2018: pH_T=7.89±0.04, temp=7.2 ± 0.5°C; summer 2018: pH_T=8.11±0.09, temp=11.6 ± 2.1°C; winter 2019: pH_T=*n*.a., temp=7.2 ± 0.4°C).

To measure linear growth, the coralline algae were imaged using a fluorescent lamp channel on a Ziess AxioZoom microscope at the UCSC Microscopy Center. Average growth extension from the original fluorescent stain was calculated for each individual using ImageJ (NIH v1.8.0) by analyzing measurements from up to 13 randomly selected points along the growing edge of the disk (*Crusticorallina* spp.) or from up to 17 randomly selected apical fronds in the floret (*B. orbigniana*). Growth data from the two winter season deployments were not significantly different for either coralline morphotype, and thus were pooled for analysis for each morphotype. Length extension (mm d^{-1}) was compared between seasons for each morphotype and between morphotypes using one-way Welch's ANOVAs (package "stats" in R [85]) due to inequality of variance and unbalanced design - a result of high variation in final sample size among deployments following random losses in the field as well as inconsistent fluorescent stain uptake (*B. orbigniana* summer, $n = 13$; *B. orbigniana* winter, $n = 34$; *Crusticorallina* spp. summer, $n = 7$; *Crusticorallina* spp. winter, $n = 25$). Adjusted p-values for these analyses were calculated using Bonferroni corrections for multiple comparisons.

2.4. Ocean acidification laboratory experiment

To test the response of the *Crusticorallina* spp. and *Bossiella orbigniana* to future OA scenarios, we used an 18-aquaria indoor experimental system with flow-through seawater at the Sitka Sound Science Center to simulate three static pH_T levels (current summer = 8.0, future summer/current winter = 7.7, future winter = 7.4) under two seasonal light regimes simulated with full-spectrum aquarium lights (AI Prime HD) (summer = PPFD 55 μmol m^{-2} s^{-1}, 13 h d^{-1}, winter = PPFD 40 μmol m^{-2} s^{-1}, 6 h d^{-1}). We had a total of 3 aquaria for each of the 6 treatment combinations (Fig. A.2). Experimental pH levels were chosen to reflect current seasonal minimums of coastal pH measured at Harris Is. from 2016 to 2017 [12], as well as end-of-century projections for Gulf of Alaska pH levels based on RCP 8.5 (−0.3 pH_T from current levels [86]). Experimental light regimes were defined using seasonal averages for day length and measured irradiance level at 10 m depth at Harris Is. (described in Section 2.1). Our experimental system was not designed to control for temperature; seawater in all aquaria followed natural temperature variation in the system's seawater source throughout the experiment. A full description of the pH control for this system can be found in Kroeker et al. [12], but in short: pH was regulated using a relay system that controlled mixing of pre-equilibrated low-pH seawater (formed by bubbling pure CO_2 gas into seawater: pHE6.0) and ambient pH seawater into 9 header buckets ($n = 3$ headers per pH treatment) that then flowed into the experimental aquaria. Each header bucket was equipped with a pH sensor (DuraFET, Honeywell) communicating with a controller (UDA 2152, Honeywell) to regulate flow of the low pH water through solenoid valves to maintain pre-programmed pH setpoints. The layout of our experiment was designed to minimize spatial variance among the random factors, aquaria and headers, by randomizing treatment assignments and relative locations throughout the system.

Within each pH level and light treatment combination, half of the individual *Crusticorallina* spp. and *B. orbigniana* were randomly assigned to be paired in close proximity with *Cryptopleura ruprechtiana* ($n = 6$ species $treatment^{-1}$), a dominant subcanopy-forming fleshy red alga in Sitka Sound frequently found growing in association with coralline algae. All algal individuals were collected on Aug 5, 2017 at Marshall Is., Sitka Sound, and cleaned using the same methods as described in Section 2.3. Algal individuals were then elevated off the bottom of experimental aquaria using PVC stands topped with plastic mesh (see Fig. A.2B). Total experimental duration was 45d (Aug 7-Sept 21, 2017). To monitor treatment conditions, we used a handheld meter (YSI) to take daily temperature readings in the replicate aquaria and measure salinity of incoming seawater daily just upstream of our experimental system. Additionally, discrete water samples were collected from replicate aquaria at four timepoints (Aug 18, 22, 25, and Sept 15) for determination of pH (total scale) and total alkalinity (TA). Discrete samples were collected without aeration in amber glass bottles, immediately poisoned with saturated $HgCl_2$ (0.025% $volume^{-1}$), and capped to prevent air exchange.

Discrete water samples for laboratory measurements of pH and/or TA were transported to UCSC for analysis within 8 months of collection. We measured pH spectrophotometrically (Shimadzu, UV-1800) using m-cresol purple dye following best practices [87], with an average standard error of ±0.0013 pH units among sample triplicates. TA measurements were performed using open cell titration (Metrohm, 905 Titrandro) and

corrected against certified reference materials of CO_2 in seawater (Dickson laboratory, Scripps Institution of Oceanography), with an average standard error of ±0.933μmol kg^{-1} SW^{-1} among sample triplicates. To calculate pH_T in the replicate aquaria at the time of water sampling, we used our measurements of spectrophotometric pH, TA, temperature, and salinity, as well as the dissociation constants [88,89] as inputs to the program CO2SYS [90].

2.4.1. Algal net calcification and growth

The effects of each experimental pH and light treatment combination and fleshy red algal association on coralline net calcification rate were assessed using the buoyant weight technique [91], as well as the alkalinity anomaly technique. To determine total relative change in calcified mass over the experimental period, each coralline thalli's buoyant weight was measured to the nearest 0.0001 g at the beginning and end of the experiment on a balanced platform suspended below a microbalance in a temperature-monitored seawater bath. All fouling organisms were removed prior to taking measurements. To ensure precision, buoyant weights were repeated for each individual until measurements differed by less than ±0.005 g, and then an average was taken of the measurements falling in this range of precision. Initial and final buoyant weights (BW; g) were used to calculate relative net calcification rate (RCR_{net};% change in BW d^{-1}) of each individual alga using the equation:

$$RCR_{net} = \frac{log\left(\frac{BW_{final}}{BW_{initial}}\right) \cdot 100}{\Delta t}$$

where Δt (d) is the total days elapsed between the beginning and end of the experiment.

Total alkalinity (TA) incubations were run in the last week of the experiment on a subset of coralline algae from each treatment (n = 3 individuals treatment^{-1} species^{-1}) by isolating individuals in 245 mL glass chambers filled with seawater from their associated aquaria and sealed airtight. Paired *C. ruprechtiana* were not included in incubation chambers, in order to isolate the physiological responses of the coralline algae. Chambers were placed on a magnetic stir plate in a water bath at consistent temperature (13°C), with stir bars able to spin freely underneath coralline algae separated by a mesh screen. All incubations were run under a mean PPFD of 80 μmol m^{-2} s^{-1} for 3 h. At the end of the incubation period, seawater from each chamber was collected to measure endpoint TA. Seawater for TA incubation chamber controls was collected from corresponding aquaria at the beginning of each incubation round and used to measure any background TA variation in empty chambers during the incubation period. All discrete water samples for TA were poisoned and processed as outlined in Section 2.4.

TA measurements from coralline algal incubations were used to calculate short-term net calcification (G_{net}; μmol g^{-1} DW h^{-1}) using the equation:

$$G_{net}(CaCO_3) = \frac{\Delta TA \cdot v}{2 \cdot DW \cdot \Delta t}$$

where ΔTA (μmol kgSW^{-1}) is the change in total alkalinity from the beginning to end of the incubation period corrected to chamber controls, v (L) is the chamber volume, DW (g) is the dry weight of the alga, and Δt (h) is the total incubation time [49,92]. Dry weights (DW; g) for the living coralline thalli used in TA incubations were estimated from buoyant weight (BW; g) measurements using the equation [91]:

$$DW = \frac{BW}{1 - \left(\frac{\rho_{SW}}{\rho_{calcite}}\right)}$$

where we used a seawater density (ρ_{SW}) of 1.02 g cm^{-3} (from average temperature and salinity data at the time of BW) and a calcite density ($\rho_{calcite}$) of 2.71 g cm^{-3}.

Growth rates of *C. ruprechtiana* reared in association with coralline algae in the different treatment conditions were quantified by measuring tissue wet weights (WW; g) at the beginning and end of the experiment. Thalli were removed from seawater, patted uniformly dry, and immediately weighed on a standard microbalance to the nearest 0.0001 g. Relative growth rate (RGR_{net};% change in WW d^{-1}) of each individual alga was calculated using the equation:

$$RGR_{net} = \frac{log\left(\frac{WW_{final}}{WW_{initial}}\right) \cdot 100}{\Delta t}$$

where Δt (d) is the total days elapsed between the beginning and end of the experiment.

We quantified variability in experiment-integrated relative net calcification rate and short-term net calcification rate of each coralline morphotype using linear mixed-effects models (package "lme4" in R [85]) with pH, *light regime,association with C. ruprechtiana, and all of the interactions between these factors* as fixed factors and *experimental aquaria* nested in *header* as random intercepts using restricted maximum likelihood. Variability in the relative growth rate of *C. ruprechtiana* was analyzed using a similar model, except fixed factors were only pH, *light regime, and* pH**light regime*. All models satisfied assumptions of normality and homoscedasticity. We determined p-values for the effects of fixed factors and their interactions using the Sattertwaithe's method for t-tests (package "lme4" in R [85]). Post-hoc tests of pairwise differences among means of significant factors were performed using the Tukey method of multiple comparisons (package "multcomp" in R [85]).

2.4.2. Experimental photophysiology

In vivo photophysiology was characterized for all red algal species at the end of the experiment by measuring the rate of oxygen evolution produced by algal thalli at seven irradiance levels. Following the final buoyant mass measurement, a small piece of thallus (mean ± SE: *B. orbigniana*: 0.17±0.02 g; *Crusticorallina* spp.: 0.53±0.03 g; *C. ruprechtiana*: 0.07±0.003 g) was taken from haphazardly selected individuals (n = 3 treatment^{-1} species^{-1}) and placed in a 69 mL incubation chamber filled with seawater from the associated aquaria and equipped with a stir bar and an oxygen sensor spot (PreSens SP-PSt4-SA). Sensor spots were calibrated daily using a two-point correction of 100% (air-saturated water) and 0% (1% Na_2SO_3 and 0.05% $Co(NO_3)_2$ standard solution) saturation. Incubation chambers were sealed airtight using clear plexiglass lids affixed with vacuum grease and submerged onto a magnetic stir plate in a temperature-controlled water bath. Full-spectrum aquarium lights (AI Hydra HD) were used to expose thalli in chambers to seven consecutively increasing irradiance levels (~PPFD 0, 20, 70, 140, 320, 425, 720 μmol m^{-2} s^{-1}). A fiber optic O_2 sensor (Fibox IV, Presens) was used to record the dissolved oxygen concentration in each chamber at 30, 45 and 60 min after each irradiance level was reached. Chamber seawater was refreshed after the fourth irradiance step to avoid nutrient depletion and oxygen supersaturation. Dissolved oxygen evolution rate (mg O_2 min^{-1}) at each irradiance level was calculated using linear regression, corrected against paired chamber controls (no algae), and normalized to chamber volume and thalli wet mass.

We used nonlinear regression models (package "nlstools" in R [85]) to mathematically fit our calculations of algal oxygen evolution rate by irradiance level to photosynthesis-irradiance (P-E) curves using the double exponential decay function:

$$NP = P_{max} \cdot \left(1 - \frac{-\alpha \cdot I}{e^{Pmax}}\right) \cdot \frac{-\beta \cdot I}{e^{Pmax}})$$

where NP = net production (mg O_2 g^{-1} min^{-1} L^{-1}), P_{max} = maximum photosynthetic rate that could be sustained with no photoinhibition (β=0), α = photosynthetic efficiency parameter (initial slope), β = photoinhibition parameter, I = irradiance level (μmol m^{-2} s^{-1}) [93]. Nonlinear least squares estimates for parameters P_{max}, α, and β were calculated for each coralline morphotype by treatment combination by fitting the above model to pooled photophysiology data from treatment replicates and performing an iterative estimation procedure assuming normal distributions. Validity of model fit was visualized by superimposing the fitted curves over the raw data and assessing estimated standard errors and t-test statistics for the estimated parameters.

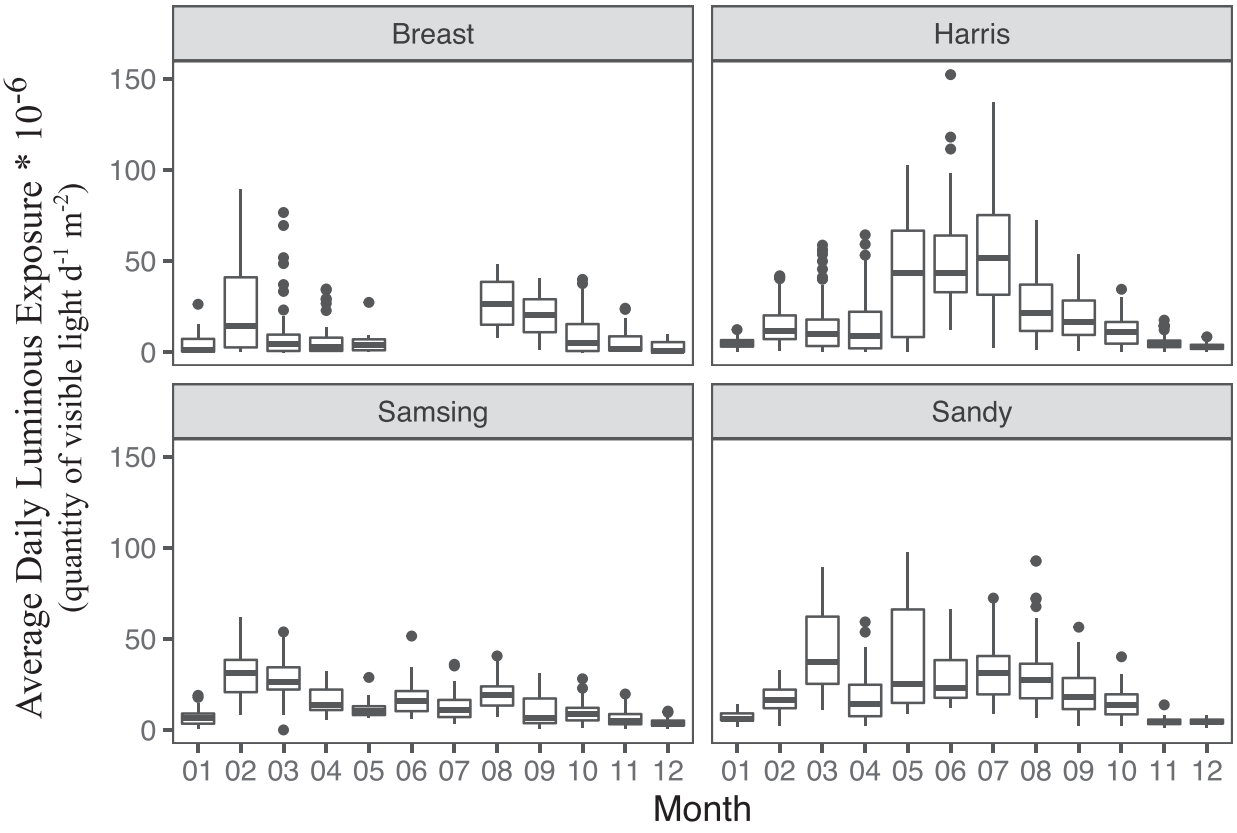

Fig. 1. Average daily luminous exposure at the benthos (~7 m MLLW) at four rocky reef monitoring sites in Sitka Sound, Alaska. Boxplots represent data averaged by calendar day across 4 years (2017–2020), summarized by month.

The effect of pH on individual parameters was determined by testing whether the addition of a binary parameter differentiating pH treatment to the model significantly altered any of the estimates for P_{max}, α, and β. Where pH was found to have a significant impact on optimal model parameters, accuracy of this estimated effect was assessed by visually comparing 'goodness of fit' of the predicted model containing the pH parameter to the original model fitted to the empirical data.

3. Results

3.1. Subtidal light availability

Average daily luminous exposure (lumens d^{-1} m^{-2}) reaching the benthos at all four monitoring sites between 2017 and 2020 (Fig. 1) was lowest in late fall and early winter (Oct - Jan). At three of the four sites, site-specific monthly averages of luminous exposure at the benthos in the late winter (Feb-Apr) were similar or higher than averages of luminous exposure recorded in the summer months (May-Aug). At all sites, average ranges of PPFD measured at the benthos during moderately overcast days typical of Southeast Alaska were very similar between winter (10–40 μmol m^{-2} s^{-1}) and summer (10–60 μmol m^{-2} s^{-1}) months.

3.2. Seasonal growth rate of coralline algae

Our results indicate that the average length extension rate of *B. orbigniana* was marginally faster in the summer (0.06±0.03 mm d^{-1}) than in the winter (0.04±0.01 mm d^{-1})(p = 0.054; Fig 2, Table A.2). We did not detect a seasonal difference in average length extension rate for *Crusticorallina* spp. (p = 1.000). Annual average length extension rates of *B. orbigniana* (0.04±0.02 mm d^{-1}) were significantly faster than annual growth rates of *Crusticorallina* spp. (0.02±0.01 mm d^{-1}; p<0.001).

3.3. Ocean acidification laboratory experiment

Treatments were maintained at setpoint targets for pH_T under our assigned winter or summer light regime for the duration of the experiment, and discrete water samples taken from experimental aquaria confirmed that seawater pCO_2 and calcite saturation state also differed by treatment (Table 1). Temperature, salinity and total alkalinity remained stable in all treatments. Temperatures during the experiment (13.6 ± 0.7°C) are representative of typical late summer (Aug-Sept) temperatures observed at Harris Is. reef in Sitka Sound (~14°C) [12].

3.3.1. Algal net calcification and growth

RCR_{net} differed by pH treatment in both *B. orbigniana* (p<0.001;Table A.3) and *Crusticorallina* spp. (p<0.001; Table A.4) (Fig. 3). Coralline algae grown under pH 7.4 (future winter scenario) experienced net dissolution (i.e., RCR_{net} < 0), regardless of light regime or close association with *C. ruprechtiana*. For both coralline algal morphotypes, only this lowest pH treatment (7.4) resulted in a significant decrease in RCR_{net} compared to a current summer scenario of pH 8.0 (p<0.001). RCR_{net} of *Crusticorallina* spp. under a future winter scenario of pH 7.4 was also lower than in the current winter scenario of pH 7.7 (p<0.001). For *Crusticorallina* species, there was an interaction between light regime and association with *C. ruprechtiana* on RCR_{net} (p = 0.024). Pairwise comparisons indicated that *Crusticorallina* spp. individuals raised under a summer light regime had lower RCR_{net} when paired with *C. ruprectiana* than when reared independently (p = 0.05), and that RCR_{net} of *Crusticorallina* spp. not paired with *C. ruprectiana*

Table 1
Seawater carbonate chemistry data (mean ± SD) by treatment over the duration of the 2017 laboratory experiment. Temperature and salinity were measured daily using a handheld meter (YSI) in all experimental aquaria (temperature) or just upstream of inflow to the experimental system (salinity). Discrete water samples were collected within each aquaria at the beginning and end of the experiment plus at least one mid-point (n = 3–4 aquaria^{-1}) for measurement of pH_T and total alkalinity (TA), and pCO_2 and saturation state (Ω) of calcite were calculated from measured parameters.

Treatment	Current summer pH	Current winter pH	Future winter pH
Temperature (°C)	13.6 ± 0.7	13.6 ± 0.7	13.6 ± 0.7
Salinity (ppt)		29.5±1.7	
pH_T	7.99 ± 0.06	7.70 ± 0.05	7.40 ± 0.03
pCO_2 (µatm)	437 ± 76	919 ± 125	1904 ± 172
TA (µmol kg^{-1})	2105 ± 14	2100 ± 11	2100 ± 17
Ω calcite	2.81 ± 0.36	1.51 ± 0.21	0.79 ± 0.06

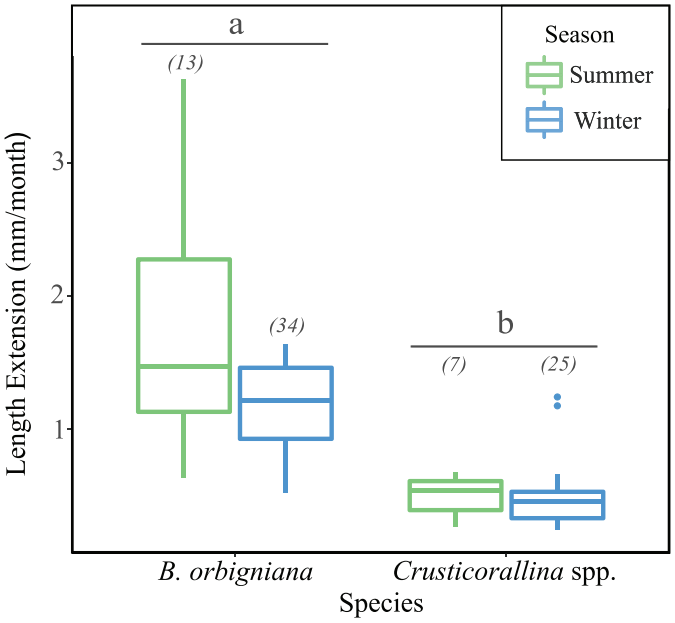

Fig. 2. Mean field growth as the rate of seasonal linear length extension for common species of coralline algae on a rocky reef (Harris Is.) in Sitka Sound, Alaska. Italicized numbers in brackets indicate sample size per group, and lowercase letters denote statistically significant differences among season and species.

was marginally lower when individuals were raised under winter light compared to summer light, although this latter comparison was not statistically significant (p = 0.077).

Short-term net calcification (G_{net}) of *B. orbigniana* (Fig. 4A) was reduced with pH (p = 0.004; Table A.5). G_{net} was lower in *B. orbigniana* thalli grown at pH 7.4 compared to thalli grown at pH 7.7 (p = 0.003). However, no difference was observed between G_{net} of thalli maintained at pH 8.0 compared to other treatments. *B. orbigniana* paired with *C. ruprechtiana* in experimental aquaria had higher G_{net} during incubations (p = 0.024), but there was no interaction between algal association and pH treatment. We did not detect an effect of pH or association with *C. ruprechtiana* on the G_{net} of *Crusticorallina* spp., and light regime had a marginal but not statistically significant effect on the crustose species' G_{net} (p = 0.074; Table A.6)(Fig. 4B). In contrast to RCR_{net} (buoyant weight technique), G_{net} (alkalinity technique) remained net positive regardless of pH treatment for all coralline algal species.

RGR_{net} of *C. ruprechtiana* over the duration of the experiment was lower under winter light regime in all pH treatments (p = 0.039; Table A.7), with no interaction between pH and light regime (Fig. A.3).

3.3.2. Experimental photophysiology

We did not detect any effect of pH treatment, light regime, or association with *C. ruprechtiana* on the photosynthetic parameters of the coralline algal species' P-E curves (p > 0.05). Photophysiology data for the coralline algal species were pooled across treatments to generate parameter estimates for average P-E curves for the two morphotypes (Fig. 5; Table A.8). We did detect a highly significant effect of pH on *C. ruprechtiana* P_{max} (p<0.001; Tables A.9 and A.10), with individuals exhibiting more than a 50% increase in this photosynthetic parameter at pH 7.4 compared to pH 8.0, regardless of light regime.

4. Discussion

Our results indicate that in the absence of evolutionary adaptation [94,95], the end-of-century projection for winter seawater pH and calcite saturation state in the Gulf of Alaska could lead to net dissolution of the encrusting *Crusticorallina* species and of the geniculate species *Bossiella orbigniana*. Understanding how concurrent changes in temperature will influence this outcome is a critical next step. Compared to the effects of seasonal variation in light availability and association with a non-calcified macroalgal species, pH and saturation state had a more pronounced impact on coralline algal calcification and thus may be more important in mediating the physiological response of these calcified algae in the future [31]. Although many species of fleshy macroalgae found in close association with coralline algae - such as the red alga *Cryptopleura ruprechtiana* considered in this study - exhibit enhanced photosynthetic rates under future ocean pCO_2 levels [36,96], increased production for one macrophyte does not necessarily confer benefits or refuge to another [e.g., 20,66,70]. Future dissolution of these foundational coralline algal species could have profound consequences for the productivity, biodiversity, and community structure of temperate rocky reefs by altering their competitive interactions with other macroalgae and reducing settlement cues and refuge habitat for invertebrate larvae and adults. At a broader level, this research highlights the importance of testing whether local variability and interactions of abiotic and biotic factors in functioning ecosystems will impact the vulnerability of specific species to global change drivers such as OA.

Although we recorded positive growth via linear tissue extension during field outplants in both summer and winter seasons, month-long laboratory simulations suggested that net calcification of coralline algal species grown in current winter pH conditions, albeit at higher temperatures than experienced in the field, may already hover near zero (Fig. 3). As noted, discrepancies between our *in-situ* versus experimental growth rates may have arisen due to differences in temperature and pH conditions during field deployments compared to conditions in experimental aquaria, and because of logistical constraints preventing our use of directly comparable methods. For example, the average temperature used in the lab simulations was 6.4°C higher than the average temperature

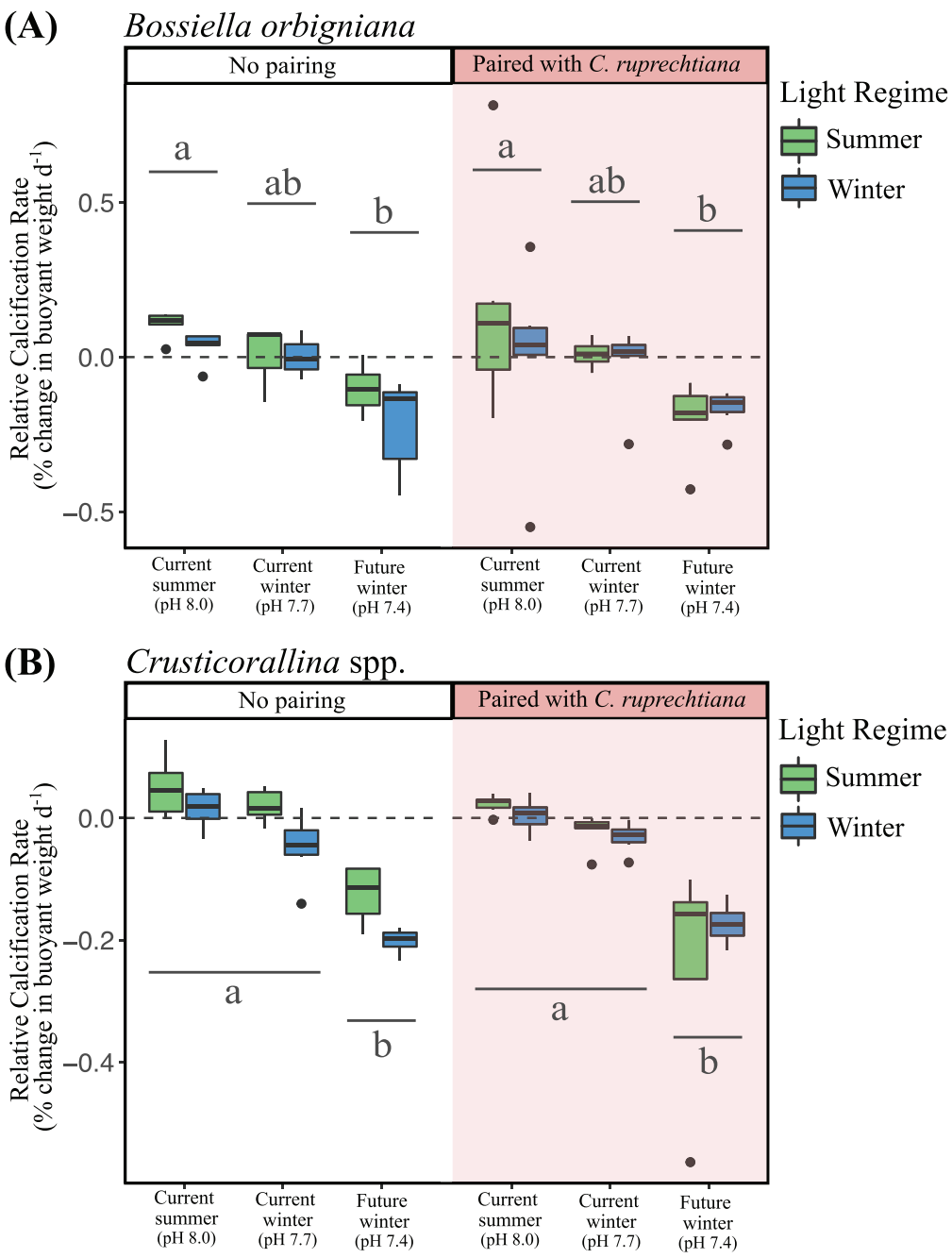

Fig. 3. Relative net calcification rates (RCR_{net}) of *B. orbigniana* (A) and *Crusticorallina* spp. (B) exposed to different treatment combinations of pH, seasonal light regime, and association with a non-calcified alga (*C. ruprechtiana*) during a month-long laboratory experiment (n = 6 individuals treatment^{-1}). Lower case letters denote significant pairwise differences among pH treatment levels.

measured during the winter field outplant experiment, which may have altered the effects of low pH on coralline algal physiology [31]. Additionally, our technique for measuring growth via linear extension may not necessarily correlate with net calcification, as coralline algae can alternate their energetic investment in cellular size versus calcification [97–100], particularly in regions with high seasonality [53]. Our data suggest there is an overall decreasing trend in coralline algal net calcification with decreasing pH that may not have been detectable among all pH treatments given our sample size. Considering the net dissolution observed in both coralline algal morphotypes under simulated future winter pH conditions, future summer pH conditions will need to be consistently favorable to calcification and growth for these coralline algal species to achieve positive net calcification over the course of the year. Our laboratory results indicate that the anticipated shift in carbonate chemistry with OA that will decrease saturation state and bring future summer pH to the level of current winter pH (7.7) is likely to jeopardize this favorable seasonal window for calcification.

Short-term net calcification of experimental coralline algae during incubations revealed slightly different patterns than were seen in net calcification over the full experiment duration. Although all of the coralline species assigned to the lowest pH treatment (7.4) exhibited the lowest short-term net calcification, average calcification remained net positive in all treatments during the incubations. This is in contrast to the net dissolution observed over the month-long experiment in coralline al-

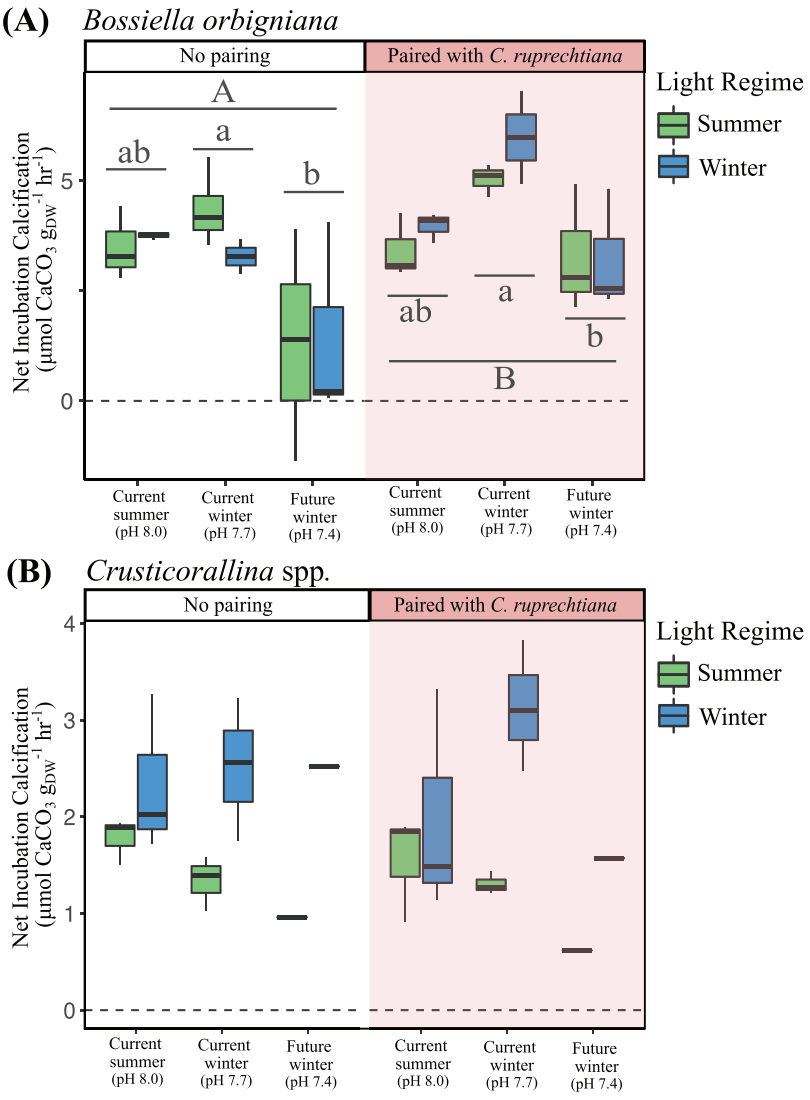

Fig. 4. Short-term net calcification rates (G_{net}) of both *B. orbigniana* (A) and *Crusticorallina* spp. (B) during 3hr total alkalinity (TA) incubations under continuous light. Data are summarized based on the assigned treatment conditions of pH, light regime, and association with a non-calcified alga (*C. ruprechtiana*) that each coralline was exposed to prior to TA incubations (n = 3 individuals treatment^{-1}). Lower case letters denote significant pairwise differences among pH treatment levels, while upper case letters denote differences between association treatments.

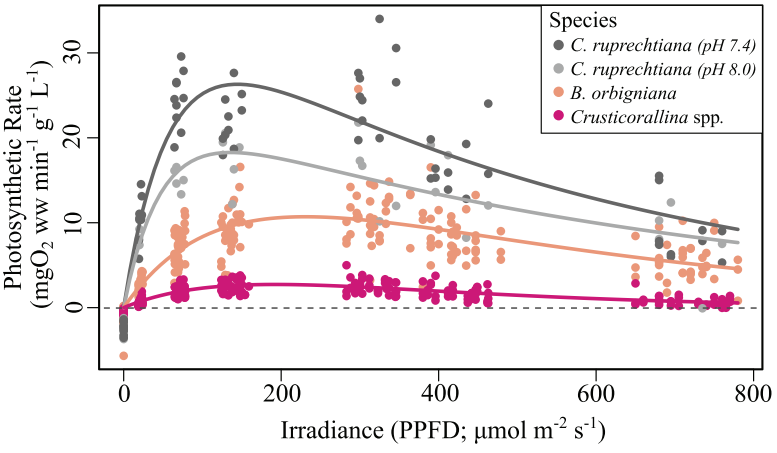

Fig. 5. Mean photosynthesis-irradiance (P-E) curves (lines) generated from repeated oxygen evolution rate measurements (circles) at multiple irradiance levels for three red algal species-groups (n = 36 individuals species^{-1}). P-E curves for coralline algal species *B. orbigniana* and *Crusticorallina* spp. are shown pooled across all experimental treatments, whereas photophysiology data for the non-calcified alga *C. ruprechtiana* are indicated separately by pH treatment.

gae assigned to the same pH 7.4 treatment. Unlike the net calcification rates integrated over experiment-long conditions, which exposed coralline algae to diel cycles of light and dark, these short-term incubations were run continuously in the light - effectively isolating the ability of these coralline algae to maintain net calcification during photosynthesis. Thus, the combined results from experiment-integrated and short-term net calcification calculations suggest that the detrimental effects of pH 7.4 conditions on coralline algal calcification are driven by dissolution under nighttime respiration, which effectively overwhelm the reduced levels of daytime calcification at low pH [52,101]. Our results also indicate that these coralline species will not be able to leverage any enhanced photosynthesis under increased pCO_2 conditions to aid in daytime calcification in the future. The absence of a low pH or high pCO_2 effect on coralline photophysiology parameters in this study is consis-

tent with observations in other coralline algal species that are confirmed to use carbon-concentrating mechanisms, such that they are not carbon-limited under current seawater conditions [102–104].

We did not detect an effect of seasonal light regime on the calcification of *B. orbigniana*, nor on the photophysiology of either morphotype, although numerous studies have shown light availability to be a major driver of coralline response to OA in other systems [13,14,16,105]. In contrast, net calcification of *Crusticorallina* spp. raised under a summer light regime decreased when these individuals were paired with (and potentially shaded by) a *C. ruprectiana* alga, which may reflect an effect of light on the growth of these crustose coralline algae. Additionally, low light acclimation may be responsible for the increase in short-term net calcification rate of *B. orbigniana* individuals shaded by *C. ruprechtiana* in experimental tanks, as well as a possible (but not statistically significant) increase in short-term calcification rate of winter light-acclimated crustose coralline algae. In these instances, we suspect that reduced light transmission through the incubation chambers may have favored low-light acclimated individuals. Increased replication within our treatment groups would have enabled a more statistically robust consideration of the effect of light. It is also important to note that while our light regime treatments differed considerably in simulated photoperiod (summer: 13 h d^{-1}, winter: 6 h d^{-1}), maximum irradiance levels as measured by photosynthetic photon flux density (PPFD) did not differ markedly between the treatments (summer: 55 μmol m^{-2} s^{-1}; winter: 40 μmol m^{-2} s^{-1}). Considering the similarity in modeled oxygen evolution rate at these irradiances in the P-E curves generated for each coralline species-group (Fig. 5), the two seasonal light regime treatments may simply not have been distinct enough to promote detectable differences in coralline photosynthetic response within our experimental design.

The varied effects of simulated seasonal light regimes on coralline algal net calcification in the lab raises the question of whether seasonal differences in light availability reaching the benthos in the field truly differ enough to modulate coralline algal response to future OA. Benthic irradiance data indicate that 24 h totals of luminous exposure (Fig. 1) and PPFD reaching the seafloor may not be as seasonally distinct as previously assumed, or at the very least, are inconsistent among sites. The high seasonal productivity in this system may influence this pattern: although total day lengths are shorter in the winter months, water column productivity and macroalgal canopy biomass over rocky reefs are relatively low [12], resulting in clearer waters and reduced canopy shading that could facilitate higher transmission of light to the benthos. In contrast, summer months are characterized by high planktonic productivity and lush canopies of fast-growing non-calcified algae, such as the subcanopy-forming fleshy red alga *C. ruprechtiana* that demonstrated enhanced growth under a summer light regime (Fig A.3). In terms of the total PPFD reaching an alga's thallus over the course of a day, the reduced light transmission to the seafloor in the summer may offset the greater number of total daylight hours in this season. This could lead to similar if not higher levels of average relative light intensity over a 24 h period in the winter season - particularly at sites with canopy-forming kelps. We observed such a pattern in our field irradiance data, where the site with the highest density of canopy-forming kelps (Samsing Pinnacle) experiences monthly maximums in luminous exposure in February and March, whereas the site with the lowest kelp densities (Harris Is.) experiences maximum luminous exposure values from May to July.

Although research on global change impacts to marine macrophytes has been limited in this region, the net productivity of non-calcified seaweeds is generally anticipated to either increase or show no change under future warming and OA [33,106]. Thus, the extent of seasonal shading caused by canopy-forming species may remain similar or intensify in the future. While the maximum photosynthetic rate of the red alga *C. ruprechtiana* increased under the future winter pH conditions, this did not translate to a detectable change in thallus wet weight; instead, this species may have allocated its enhanced carbon reserves under low pH conditions to other biological activities, such as the accumulation of sugars, polysaccharides and amino acids [107,108]. The absence of a consistent effect of fleshy red algal association on coralline algal calcification was possibly due to inconsistencies in the amount of shading among each coralline-*Cryptopleura* pairing (see Fig. A.2B), rather than an indication that shading by other canopy-forming macroalgal species is not relevant to coralline algal physiology. According to the P-E curves generated for the coralline algae, current average irradiance levels in the field fall below the light intensity at which these species exhibit maximum photosynthetic rates. Consequently, any decrease in light availability reaching the benthos resulting from enhanced productivity of canopy-forming macroalgae under future OA and warming [106,109] will theoretically lead to a reduction in coralline algal photosynthetic capacity. Additionally, our results suggest that even in close association with a non-calcified alga experiencing enhanced photosynthetic rates under OA conditions, coralline algae do not benefit from this localized draw-down of CO_2 nor from any canopy-related flow attenuation that could have altered calcification dynamics across their diffusion boundary layers [65]. It is possible that the effect of fleshy red algae on coralline algal calcification could differ based on variation in benthic flow. Unfortunately, we did not account for this variable in our study design. While standard flow rates in this experimental system are 2–3 L/min, we did not measure within-aquaria flow during this study, and we have not measured in situ flow rates on subtidal rocky reefs of this region. Yet, our results are consistent with studies demonstrating variable or negligible benefits of canopy-forming algae on benthic organism calcification [19,59]. We anticipate that the resilience of these coralline algal species to OA in this high-latitude, light-limited benthic environment will not be radically improved via their physical associations with other, non-calcified macroalgae.

Our laboratory study successfully simulated ecologically-relevant combinations of current and projected pCO_2 and light regime in Sitka Sound, yet it is important to note that we were unable to manipulate another critical environmental variable that will shift with global climate change: temperature [110]. Ocean warming is anticipated to adversely affect the photophysiology and calcification of some coralline algae, and the effect of future temperature increases may exacerbate the effects of increasing pCO_2 on coralline dissolution [111–113]. While the temperature range observed in all aquaria over the course of the experiment reflects conditions that these coralline algae naturally experience in late summer (Aug-Sept) in Sitka Sound [12], such temperatures exceed what would be expected within the scenarios simulated with our study's pCO_2 and light regime treatments. Because seasonal variation in temperature and pH in this system are not synchronous [12], this seasonal maximum in temperature does not align temporally with the annual pCO_2 extremes that this study's treatments were based upon. As a consequence, our results may overestimate the effects of pCO_2 and light regime on coralline physiology and calcification for each scenario [111]. Then again, in a recent synthesis of coralline algal research that considered the interactive effects of OA and increased temperatures, the majority of included studies found that OA was the more dominant driver of coralline algal response and that the addition of temperature did not change the effect of OA on coralline algal physiology [31]. Future research will need to address the impact of temperature on the physiology of these high-latitude coralline algal species in order to assess the contribution of this driver and its interaction with other global change stressors.

Crustose and geniculate coralline algae found within the same coastal systems often differ in overall rates of production and calcification [35,112,114], which may reveal disparate vulnerabilities to future OA between these two morphological forms. Comparing the two morphotypes considered in this study, the geniculate form (*B. orbigniana*) exhibited higher photosynthetic capacity, field length extension rates, and net calcification rates than the crustose form (*Crusticorallina* spp.). These differences between the two morphotypes, combined with the overall lower light adaptation of the crustose individuals, may lead to higher susceptibility of crustose coralline algae to corrosion under OA and a higher potential for thallus breakage under stress in this sys-

tem [115]. Combined with decreased growth rate as OA progresses, this may rapidly affect crustose species' ability to compete for space at the benthos with geniculate coralline algae and could lead to shifts in the structure and biodiversity of coralline algal assemblages [31,116].

Ultimately, if coralline algal dissolution outpaces calcification throughout the year at high latitudes under future global change scenarios, both encrusting and geniculate species considered in this study will be vulnerable to increased competition for space by non-calcified macroalgae [31,32,38,39,117]. The diverse and essential roles that coralline algae play in temperate rocky reef systems - as foundational reef structure, year-round primary producers and carbon reservoirs, and settlement habitat for associated invertebrates [35] - will shift with changes in their relative biomass. Ecological research considering the long-term community-level consequences of a reduction or absence of macrophyte calcifiers across a diversity of marine systems should continue to be prioritized if we seek to effectively anticipate the bottom-up effects on coastal ecosystem function across the world.

5. Conclusion

This study confirms the vulnerability of two spatially dominant, yet previously unstudied morphotypes of calcium carbonate containing algae in the northern Pacific to end-of-century projections of OA in this region. While high-latitude coralline algae already experience annual swings in seawater carbonate chemistry of over 0.4 pH units between winter and summer seasons [12], we have confirmed that the geniculate alga *Bossiella orbigniana* and individuals from the crustose alga genus *Crusticorallina* are still able to add calcified tissue via linear extension from their meristems through both seasons in the field. In contrast, under laboratory-simulated pH conditions expected in the winter months by year 2100, both coralline morphotypes exhibited net dissolution and no change in photosynthetic performance.

Although the long daylight hours that characterize high-latitude summers might be expected to benefit coralline algal photosynthesis and calcification capacity, our results suggest that the actual difference in seasonal light availability reaching the benthos in this temperate subtidal system may not be sufficient to significantly modulate coralline algal productivity. In fact, increasing productivity and canopy-coverage by non-calcified macroalgae under future OA and warming may further reduce irradiance levels at the benthos during the summer [106]. Given that the relatively higher pH summer season may represent the only annual opportunity for coralline algae to achieve positive net calcification under future OA scenarios in this region, increased shading by closely associated algae - particularly in the absence of any ameliorating effect on local carbonate chemistry - may ultimately limit coralline algal resilience to dissolution.

Anthropogenic emissions of CO_2 and the concomitant decrease in oceanic pH and carbonate saturation state will overlay onto spatially and temporally variable, ecologically complex marine systems. This research responds to a call to incorporate seasonally dependent abiotic and biotic interactions in our consideration of vulnerable species' response to global change drivers, a challenging yet necessary approach in the coming era of climate change science that can be used to identify where and when future conditions of enhanced stress are most likely to occur. We strongly recommend that future research investigating the emergent effects of global change in marine macroalgal communities continues to consider how seasonality and other natural variability interacts with global change drivers to shape the responses of a wide diversity of co-occurring and interacting seaweed species.

Funding

This work was supported by the National Science Foundation [OCE-1,752,600], the David and Lucile Packard Foundation, the Koret Foundation, and the UCSC Maximizing Access to Research Careers (MARC) U*STAR program (NIH 2T34GM007910–38). DNA sequencing supported by a family trust to PWG.

Data linking

The data that support the findings of this study are openly available in BCO-DMO at www.bco-dmo.org, project number 756,735.

Declaration of interests

The authors declare that they have no known competing financial interests or personal relationships that could have appeared to influence the work reported in this paper.

CRediT authorship contribution statement

LE Bell: Conceptualization, Methodology, Investigation, Formal analysis, Writing – original draft, Writing – review & editing, Visualization, Project administration. **JB Gómez:** Investigation, Methodology, Formal analysis, Writing – review & editing. **E Donham:** Conceptualization, Methodology, Writing – review & editing. **DL Steller:** Conceptualization, Methodology, Writing – review & editing. **PW Gabrielson:** Investigation, Resources, Writing – review & editing. **KJ Kroeker:** Conceptualization, Methodology, Investigation, Resources, Writing – review & editing, Supervision, Funding acquisition.

Acknowledgments

We thank C. Powell and E. O'Brien (UCSC) and J. Klejka for their invaluable assistance in the field and laboratory, T. Vision (UNC, Chapel Hill) for lab space and equipment, and D. Wilson Freshwater (DNA Analysis Core Facility, Center for Marine Sciences, UNC, Wilmington) for final sequencing. We also thank P. Raimondi (UCSC) for his assistance with our linear mixed model analyses, M. Kilpatrick (UCSC) for his guidance with our photophysiology data analysis, B. Abrams (UCSC Life Sciences Microscopy Center) for his support with fluorescent imaging analysis, and the Sitka Sound Science Center staff for their diving and facilities support in Sitka.

Appendix A

Table A.1
List of voucher specimens deposited in the University of North Carolina, Chapel Hill herbarium (NCU) with accession number, collection data, and GenBank accession number of the *rbc*L 694 base pair sequence for each.

Taxon Name	Herbarium Accession No.	Collection Data	GenBank Accession No. (*rbc*L)
Bossiella orbigniana	NCU 673983	Marshall Island, Sitka, 57.031844 N, 135.272729 W, 5.viii.2017, on rock reef with *Macrocystis pyrifera*, leg. Lauren Bell	OK430853
Bossiella orbigniana	NCU 673,984	Marshall Island, Sitka, 57.031844 N, 135.272729 W, 5.viii.2017, on rock reef with *Macrocystis pyrifera*, leg. Lauren Bell	OK430852
Bossiella orbigniana	NCU 673,985	Marshall Island, Sitka, 57.031844 N, 135.272729 W, 5.viii.2017, on rock reef with *Macrocystis pyrifera*, leg. Lauren Bell	OK430857
Bossiella orbigniana	NCU 673,986	Marshall Island, Sitka, 57.031844 N, 135.272729 W, 5.viii.2017, on rock reef with *Macrocystis pyrifera*, leg. Lauren Bell	OK430855
Bossiella orbigniana	NCU 673,987	Marshall Island, Sitka, 57.031844 N, 135.272729 W, 5.viii.2017, on rock reef with *Macrocystis pyrifera*, leg. Lauren Bell	OK430854
Bossiella orbigniana	NCU 673,988	Marshall Island, Sitka, 57.031844 N, 135.272729 W, 5.viii.2017, on rock reef with *Macrocystis pyrifera*, leg. Lauren Bell	OK430858
Bossiella orbigniana	NCU 673,989	Marshall Island, Sitka, 57.031844 N, 135.272729 W, 5.viii.2017, on rock reef with *Macrocystis pyrifera*, leg. Lauren Bell	OK430859
Bossiella orbigniana	NCU 673,990	Marshall Island, Sitka, 57.031844 N, 135.272729 W, 5.viii.2017, on rock reef with *Macrocystis pyrifera*, leg. Lauren Bell	OK430860
Bossiella orbigniana	NCU 673,991	Marshall Island, Sitka, 57.031844 N, 135.272729 W, 5.viii.2017, on rock reef with *Macrocystis pyrifera*, leg. Lauren Bell	OK430861
Bossiella orbigniana	NCU 673,992	Marshall Island, Sitka, 57.031844 N, 135.272729 W, 5.viii.2017, on rock reef with *Macrocystis pyrifera*, leg. Lauren Bell	OK430856
Bossiella orbigniana	NCU 673,993	Marshall Island, Sitka, 57.031844 N, 135.272729 W, 5.viii.2017, on rock reef with *Macrocystis pyrifera*, leg. Lauren Bell	OK430862
Bossiella orbigniana	NCU 673,994	Marshall Island, Sitka, 57.031844 N, 135.272729 W, 5.viii.2017, on rock reef with *Macrocystis pyrifera*, leg. Lauren Bell	OK430863
Crusticorallina adhaerens	NCU 673,995	Marshall Island, Sitka, 57.031844 N, 135.272729 W, 5.viii.2017, on rock reef with *Macrocystis pyrifera*, leg. Lauren Bell	OK430869
Crusticorallina muricata	NCU 673,996	Marshall Island, Sitka, 57.031844 N, 135.272729 W, 5.viii.2017, on rock reef with *Macrocystis pyrifera*, leg. Lauren Bell	OK430864
Crusticorallina muricata	NCU 674,003	Marshall Island, Sitka, 57.031844 N, 135.272729 W, 5.viii.2017, on rock reef with *Macrocystis pyrifera*, leg. Lauren Bell	OK430865
Crusticorallina muricata	NCU 674,004	Marshall Island, Sitka, 57.031844 N, 135.272729 W, 5.viii.2017, on rock reef with *Macrocystis pyrifera*, leg. Lauren Bell	OK430866
Crusticorallina muricata	NCU 674,005	Marshall Island, Sitka, 57.031844 N, 135.272729 W, 5.viii.2017, on rock reef with *Macrocystis pyrifera*, leg. Lauren Bell	OK430867
Crusticorallina muricata	NCU 674,006	Marshall Island, Sitka, 57.031844 N, 135.272729 W, 5.viii.2017, on rock reef with *Macrocystis pyrifera*, leg. Lauren Bell	OK430868
Crusticorallina painei	NCU 673,997	Marshall Island, Sitka, 57.031844 N, 135.272729 W, 5.viii.2017, on rock reef with *Macrocystis pyrifera*, leg. Lauren Bell	OK430870
Crusticorallina painei	NCU 673,998	Marshall Island, Sitka, 57.031844 N, 135.272729 W, 5.viii.2017, on rock reef with *Macrocystis pyrifera*, leg. Lauren Bell	OK430871
Crusticorallina painei	NCU 673,999	Marshall Island, Sitka, 57.031844 N, 135.272729 W, 5.viii.2017, on rock reef with *Macrocystis pyrifera*, leg. Lauren Bell	OK430872
Crusticorallina painei	NCU 674,000	Marshall Island, Sitka, 57.031844 N, 135.272729 W, 5.viii.2017, on rock reef with *Macrocystis pyrifera*, leg. Lauren Bell	OK430873
Crusticorallina painei	NCU 674,001	Marshall Island, Sitka, 57.031844 N, 135.272729 W, 5.viii.2017, on rock reef with *Macrocystis pyrifera*, leg. Lauren Bell	OK430874
Crusticorallina painei	NCU 674,002	Marshall Island, Sitka, 57.031844 N, 135.272729 W, 5.viii.2017, on rock reef with *Macrocystis pyrifera*, leg. Lauren Bell	OK430875
Crusticorallina painei	NCU 674,007	Marshall Island, Sitka, 57.031844 N, 135.272729 W, 5.viii.2017, on rock reef with *Macrocystis pyrifera*, leg. Lauren Bell	OK430876
Crusticorallina painei	NCU 674,008	Marshall Island, Sitka, 57.031844 N, 135.272729 W, 5.viii.2017, on rock reef with *Macrocystis pyrifera*, leg. Lauren Bell	OK430877

Table A.2
Results from three Welch's ANOVAs comparing mean coralline algal linear extension rates (mm d^{-1}) in the field by season for each morphotype, and between morphotypes with adjusted p-values for multiple comparisons using Bonferroni corrections.

One-way test	df_{num}	df_{den}	F	Adjusted p-value
winter vs. summer *(Crusticorallina* spp.)	1	14.967	0.002	1.000
winter vs. summer (*B. orbigniana)*	1	12.957	6.213	0.054
Crusticorallina spp vs. *B. orbigniana* (seasons combined)	1	61.999	79.606	**<0.001***

Table A.3
Summary statistics from mixed linear model analysis of *B. orbigniana* relative net calcification rate over the duration of the laboratory experiment (RCR_{net}).
Formula–*B. orbigniana* RCR_{net} ~ pH * light regime * association with *C. ruprechtiana* + (1|header/aquaria).

i. *Variance components for random effects*

Groups	Variance	Std. Dev.
aquaria:header	0.000	0.000
header	0.000	0.000
residual	0.028	0.168

ii. *ANOVA results from the mixed linear model*

Source	**SS**	**MSE**	**numDF**	**denDF**	**F value**	**Pr(>*F*)**
pH	0.551	0.276	2	41	9.72	**<0.001***
light regime	0.059	0.059	1	41	2.08	0.157
C. ruprechtiana association	0.001	0.001	1	41	0.04	0.837
pH:light	0.046	0.023	2	41	0.80	0.455
pH:assoc.	0.011	0.006	2	41	0.20	0.819
light:assoc.	<0.001	<0.001	1	41	0.01	0.934
pH:light:assoc.	0.024	0.012	2	41	0.42	0.662

iii. Statistics from Tukey's post-hoc tests comparing the effects of pH levels on B. orbigniana RCR_{net}.

Condition1	**Condition2**	**estimate**	**SE**	**z value**	**Pr(>|z|)**
Current summer (8.0)	Current winter (7.7)	-0.147	0.087	−1.70	0.120
	Future winter (7.4)	-0.281	0.075	−3.73	**<0.001***
Current winter (7.7)	Future winter (7.4)	-0.134	0.087	−1.54	0.160

Number of observations: 53.
Groups: aquaria:header, 18; header, 9.

Table A.4
Summary statistics from mixed linear model analysis of *Crusticorallina* spp. relative net calcification rate over the duration of the laboratory experiment (RCR_{net}).
Formula–*Crusticorallina* spp. RCR_{net} ~ pH * light regime * association with *C. ruprechtiana* + (1|header/aquaria).

i. *Variance components for random effects*

Groups	Variance	Std. Dev.
aquaria:header	0.0001	0.010
header	0.0002	0.013
residual	0.004	0.060

ii. *ANOVA results from the mixed linear model*

Source	**SS**	**MSE**	**numDF**	**denDF**	**F value**	**Pr(>*F*)**
pH	0.263	0.132	2	4.719	36.715	**0.001***
light regime	0.007	0.006	1	4.661	1.820	0.239
C. ruprechtiana association	0.010	0.010	1	37.547	2.805	0.102
pH:light	0.002	0.001	2	4.636	0.300	0.754
pH:assoc.	0.005	0.002	2	37.488	0.634	0.526
light:assoc.	0.020	0.020	1	37.547	5.503	**0.024***
pH:light:assoc.	0.015	0.007	2	37.488	2.076	0.140

iii. *Statistics from Tukey's post-hoc tests comparing the effects of pH levels on* Crusticorallina spp. *RCR_{net}*.

Condition1	**Condition2**	**estimate**	**SE**	**z value**	**Pr(>|z|)**
Current summer (8.0)	Current winter (7.7)	−0.028	0.029	−0.97	0.350
	Future winter (7.4)	−0.205	0.033	−6.13	**<0.001***
Current winter (7.7)	Future winter (7.4)	−0.177	0.032	−5.45	**<0.001***

iv. *Statistics from Tukey's post-hoc tests comparing the effects of interactive levels of light regime and* C. ruprechtiana *association on* Crusticorallina spp. *RCR_{net}*.

Condition1	**Condition2**	**estimate**	**SE**	**t value**	**Pr(>|t|)**
summer light, no CR	winter light, no CR	0.059	0.023	2.55	0.077
	summer light, w/ CR	0.063	0.023	2.76	**0.050***
	winter light, w/ CR	0.049	0.023	2.10	0.183
winter light, no CR	summer light, w/ CR	0.004	0.023	0.17	0.998
	winter light, w/ CR	−0.011	0.022	−0.49	0.961
summer light, w/ CR	winter light, w/ CR	−0.015	0.023	−0.64	0.916

Number of observations: 61.
Groups: aquaria:header, 18; header, 9.
Note: CR = Cryptopleura ruprechtiana; w/ = paired with; no = no association.

Table A.5
Summary statistics from mixed linear model analysis of *B. orbigniana* short-term net calcification rate during total alkalinity incubations (G_{net}).
Formula–*B. orbigniana* G_{net} ~ pH * light regime * association with *C. ruprechtiana* + (1|header/aquaria).

i. *Variance components for random effects*

Groups	Variance	Std. Dev.
aquaria:header	0.000	0.000
header	0.000	0.000
residual	1.700	1.310

ii. *ANOVA results from the mixed linear model*

Source	SS	MSE	numDF	denDF	F value	Pr(>*F*)
pH	25.080	12.540	2	22	7.36	**0.004***
light regime	0.420	0.430	1	22	0.25	0.621
C. ruprechtiana association	10.05	10.040	1	22	5.89	**0.024**
pH:light	0.350	0.180	2	22	0.10	0.902
pH:assoc.	4.650	2.330	2	22	1.36	0.276
light:assoc.	0.500	0.500	1	22	0.29	0.593
pH:light:assoc.	2.660	1.330	2	22	0.78	0.471

iii. *Statistics from Tukey's post-hoc tests comparing the effects of* pH *levels on* B. orbigniana G_{net}.

Condition1	Condition2	estimate	SE	z value	Pr(>|z|)
Current summer (8.0)	Current winter (7.7)	1.239	0.730	1.70	0.999
	Future winter (7.4)	−1.163	0.754	−1.54	0.150
Current winter (7.7)	Future winter (7.4)	−2.402	0.730	−3.29	**0.001***

Number of observations: 34.
Groups: aquaria:header, 11; header, 6.

Table A.6
Summary statistics from mixed linear model analysis of *Crusticorallina* spp. short-term net calcification rate during total alkalinity incubations (G_{net}).
Formula–*Crusticorallina* spp. G_{net} ~ pH * light regime * association with *C. ruprechtiana* + (1|header/aquaria).

i. *Variance components for random effects*

Groups	Variance	Std. Dev.
aquaria:header	0.199	0.447
header	0.130	0.369
residual	0.216	0.465

ii. ANOVA results from the mixed linear model

Source	SS	MSE	numDF	denDF	F value	Pr(>*F*)
pH	0.435	0.218	2	2.24	1.01	0.487
light regime	1.796	1.796	1	2.64	8.31	0.074
C. ruprechtiana association	0.016	0.016	1	12	0.08	0.787
pH:light	0.338	0.169	2	2.54	0.78	0.544
pH:assoc.	0.537	0.269	2	12	1.24	0.323
light:assoc.	0.107	0.107	1	12	0.49	0.496
pH:light:assoc.	0.228	0.228	1	12	1.06	0.325

Number of observations: 27.
Groups: aquaria:header, 10; header, 5.

Table A.7
Summary statistics from mixed linear model analysis of *Cryptopleura ruprechtiana* relative net growth rate over the duration of the laboratory experiment (RGR_{net}).
Formula–*C. ruprechtiana* RCR_{net} ~ pH * light regime + (1|header/aquaria).

i. *Variance components for random effects*

Groups	Variance	Std. Dev.
aquaria:header	0.000	0.000
header	0.000	0.000
residual	0.328	0.573

ii.ANOVA results from the mixed linear model

Source	SS	MSE	numDF	denDF	F value	Pr(>*F*)
pH	0.582	0.291	2	64	0.89	0.417
light regime	1.456	1.456	1	64	4.44	**0.039***
pH:light	0.914	0.457	2	64	1.39	0.256

Number of observations: 70.
Groups: aquaria:header, 18; header, 9.

Table A.8
Statistics of parameter estimates for photosynthesis-irradiance curves for *B. orbigniana* and *Crusticorallina* spp., pooled across all treatments by morphotype.

	Parameter	Estimate	SE	t-value	Pr(>|t|)
Bossiella orbigniana	Pmax	23.793	5.906	4.029	**<0.001***
	alpha	0.135	0.009	15.209	**<0.001***
	beta	0.050	0.022	2.295	**0.023***
Crusticorallina spp.	Pmax	16.918	0.421	40.170	**<0.001***
	alpha	0.039	0.002	22.090	**<0.001***
	Beta	0.070†			

Formula: Net production ~(Pmax) * (1 - exp(-((alpha) * I)/(Pmax))) * (exp(-((beta) * I)/(Pmax))).
† insufficient data to constrain beta parameter for Crusticorallina spp. Beta of 0.07 used to estimate Pmax and alpha parameters for curve fit.

Table A.9
Statistics of parameter estimates for *Cryptopleura ruprechtiana* photosynthesis-irradiance curves, by pH treatment. The final row indicates the significant effect of pH (as represented in model by parameter "C" multiplied by a binary pH_code representing pH treatment) on the Pmax parameter.

	Parameter	Estimate	SE	t-value	Pr(>|t|)
C. ruprechtiana (pH 7.4) (pH_code = 1)	Pmax	38.246	4.631	8.259	**<0.001***
	alpha	0.597	0.066	9.107	**<0.001***
	beta	0.070	0.020	3.561	**<0.001***
C. ruprechtiana (pH 8.0) (pH_code = 0)	Pmax	23.928	3.588	6.668	**<0.001***
	alpha	0.471	0.087	5.431	**<0.001***
	beta	0.035	0.014	2.478	**0.019***
pH *effect on Pmax*	*parameter "C"*	*7.232*	*1.330*	*5.439*	***<0.001****

Formula: Net production ~(Pmax+(C*pH_code)) * (1 - exp(-((alpha) * I)/(Pmax+(C*pH_code)))) * (exp(-((beta) * I)/(Pmax+(C*pH_code)))).

Table A.10
Statistics from an F test comparing modeled P-E curves for *C. ruprechtiana* by pH treatment.

	Res.df	Res. SS	df	SS	F-value	Pr(>*F*)
null model (pooled data)	101	2073.2				
model parameterized by group	98	1491.4	3	581.720	12.742	**<0.001***

Formula: Net production ~(Pmax) * (1 - exp(-((alpha) * I)/(Pmax))) * (exp(-((beta) * I)/(Pmax))).
Group parameters used for comparison: *C.ruprechtiana* (pH 7.4) & *C. ruprechtiana* (pH 8.0).

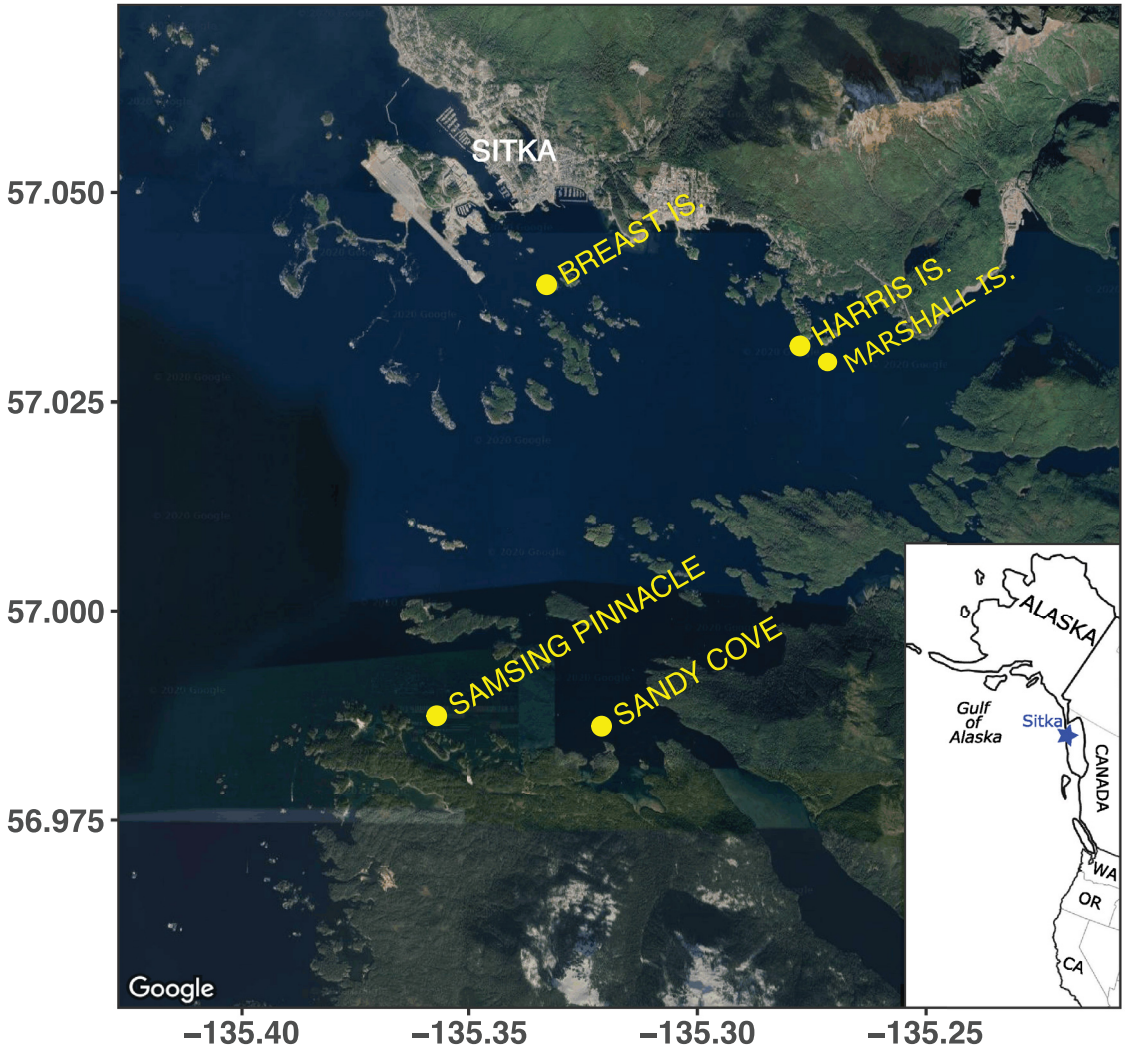

Fig. A.1. Map of rocky reef sites in Sitka Sound, Alaska used in monitoring of seasonal benthic light availability (Breast Is., Harris Is., Samsing Pinnacle, Sandy Cove; 2017–2020), collection of coralline algae for species verification and experiments (Marshall Is.), and in situ study of coralline algal growth rates (Harris Is., 2018–2019).

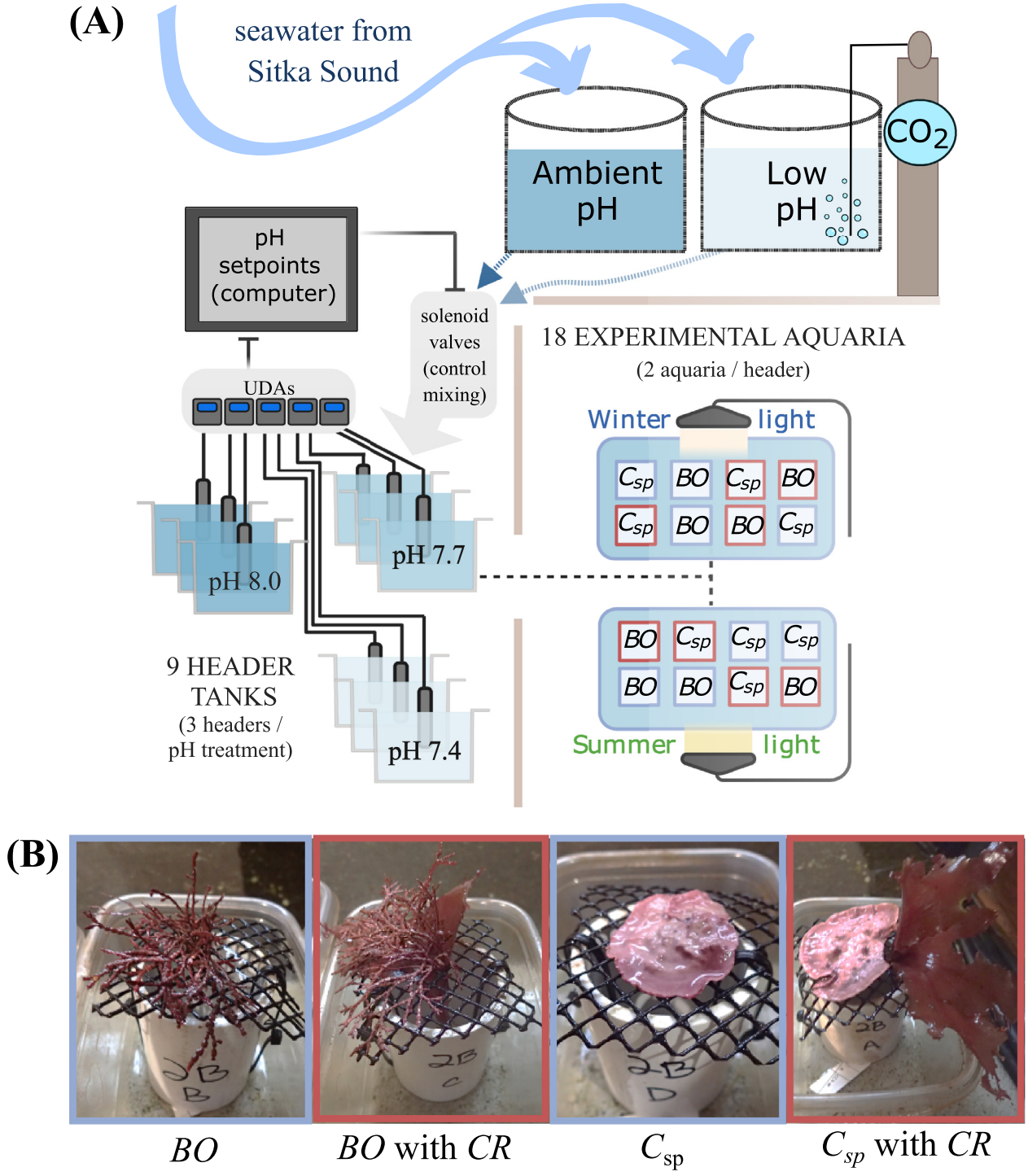

Fig. A.2. Design of the coralline algal laboratory experiment (A) and examples of individuals from either coralline algal morphotype positioned on stands with and without associated *Cryptopleura* (B). A) Incoming seawater from Sitka Sound was first routed into two main sumps, one of which was kept at ambient pH and the other was bubbled continuously with dissolved carbon dioxide gas to decrease pH. Seawater from both sumps was routed into header buckets ($n = 9$) where mixing was controlled via a feedback loop between pH sensors, controllers, and solenoid valves to achieve pre-programmed pH setpoints for experimental treatments ($n = 3$ headers/pH treatment). From each header bucket, seawater flowed into two experimental aquaria assigned either a winter or summer light regime. Each aquaria contained a random arrangement of four *B. orbigniana* ("BO") and four *Crusticorallina* ("C_{sp}") individuals, with half of the individuals within each coralline genus paired with *Cryptopleura ruprechtiana* ("CR"; indicated by red squares). B) Examples of the four within-aquaria red algal species combinations. Individuals were elevated on PVC stands (5 cm diameter) to maximize exposure to within-aquaria water flow.

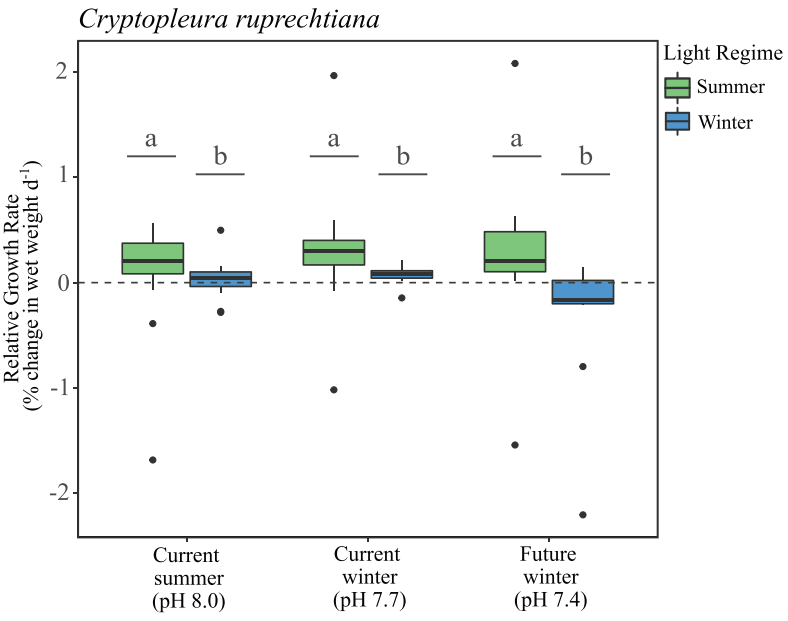

Fig. A.3. Relative growth rate (RGR_{net}) of *Cryptopleura ruprechtiana* exposed to different treatment combinations of pH and light regime during a month-long laboratory experiment (n = 12 individuals treatment^{-1}). Lower case letters denote significant differences among treatments.

References

[1] B. Helmuth, C.D.G. Harley, P.M. Halpin, M. O'Donnell, G.E. Hofmann, C.A. Blanchette, Climate change and latitudinal patterns of intertidal thermal stress, Science 298 (2002) 1015–1017, doi:10.1126/science.1076814.

[2] B.A. Menge, J. Lubchenco, M.E.S. Bracken, F. Chan, M.M. Foley, T.L. Freidenburg, S.D. Gaines, G. Hudson, C. Krenz, H. Leslie, D.N.L. Menge, R. Russell, M.S. Webster, Coastal oceanography sets the pace of rocky intertidal community dynamics, Proc. Natl. Acad. Sci. 100 (2003) 12229–12234, doi:10.1073/pnas.1534875100.

[3] E. Sanford, M.S. Roth, G.C. Johns, J.P. Wares, G.N. Somero, Local selection and latitudinal variation in a marine predator-prey interaction, Science 300 (2003) 1135–1137, doi:10.1126/science.1083437.

[4] A.J. Suggitt, P.K. Gillingham, J.K. Hill, B. Huntley, W.E. Kunin, D.B. Roy, C.D. Thomas, Habitat microclimates drive fine-scale variation in extreme temperatures, OIKOS 120 (2011) 1–8, doi:10.1111/j.1600-0706.2010.18270.x.

[5] F. Chan, J.A. Barth, C.A. Blanchette, R.H. Byrne, F. Chavez, O. Cheriton, R.A. Feely, G. Friederich, B. Gaylord, T. Gouhier, S. Hacker, T. Hill, G. Hofmann, M.A. McManus, B.A. Menge, K.J. Nielsen, A. Russell, E. Sanford, J. Sevadjian, L. Washburn, Persistent spatial structuring of coastal ocean acidification in the California current system, Sci. Rep. 7 (2017) 2526, doi:10.1038/s41598-017-02777-y.

[6] S.C. Doney, D.S. Busch, S.R. Cooley, K.J. Kroeker, The impacts of ocean acidification on marine ecosystems and reliant human communities, Annu. Rev. Environ. Resour. 45 (2020) 83–112, doi:10.1146/annurev-environ-012320-083019.

[7] G.E. Hofmann, J.E. Smith, K.S. Johnson, U. Send, L.A. Levin, F. Micheli, A. Paytan, N.N. Price, B. Peterson, Y. Takeshita, P.G. Matson, E.D. Crook, K.J. Kroeker, M.C. Gambi, E.B. Rivest, C.A. Frieder, P.C. Yu, T.R. Martz, High-frequency dynamics of ocean pH–A multi-ecosystem comparison, PLoS One 6 (2011) e28983, doi:10.1371/journal.pone.0028983.

[8] K.J. Kroeker, L.E. Bell, E.M. Donham, U. Hoshijima, S. Lummis, J.A. Toy, E. Willis-Norton, Ecological change in dynamic environments–Accounting for temporal environmental variability in studies of ocean change biology, Glob. Change Biol. 26 (2020) 54–67, doi:10.1111/gcb.14868.

[9] R.A. Feely, R.H. Byrne, J.G. Acker, P.R. Betzer, C.-T.A. Chen, J.F. Gendron, M.F. Lamb, Winter-summer variations of calcite and aragonite saturation in the Northeast Pacific, Mar. Chem. 25 (1988) 227–241, doi:10.1016/0304-4203(88)90052-7.

[10] S.A. Siedlecki, D.J. Pilcher, A.J. Hermann, K. Coyle, J. Mathis, The importance of freshwater to spatial variability of aragonite saturation state in the Gulf of Alaska, J. Geophys. Res. Oceans 122 (2017) 8482–8502, doi:10.1002/2017JC012791.

[11] C. Hauri, C. Schultz, K. Hedstrom, S. Danielson, B. Irving, S.C. Doney, R. Dussin, E.N. Curchitser, D.F. Hill, C.A. Stock, A regional hindcast model simulating ecosystem dynamics, inorganic carbon chemistry, and ocean acidification in the Gulf of Alaska, Biogeosciences 17 (2020) 3837–3857, doi:10.5194/bg-17-3837-2020.

[12] K.J. Kroeker, C. Powell, E.M. Donham, Windows of vulnerability–Seasonal mismatches in exposure and resource identity determine ocean acidification's effect on a primary consumer at high latitude, Glob. Change Biol. 27 (2021) 1042–1051, doi:10.1111/gcb.15449.

[13] B.D. Russell, C.A. Passarelli, S.D. Connell, Forecasted CO_2 modifies the influence of light in shaping subtidal habitat, J. Phycol. 47 (2011) 744–752, doi:10.1111/j.1529-8817.2011.01002.x.

[14] P.S.M. Celis-Plá, J.M. Hall-Spencer, P.A. Horta, M. Milazzo, N. Korbee, C.E. Cornwall, F.L. Figueroa, Macroalgal responses to ocean acidification depend on nutrient and light levels, Front. Mar. Sci. 2 (2015) 26, doi:10.3389/fmars.2015.00026.

[15] D. Britton, C.E. Cornwall, A.T. Revill, C.L. Hurd, C.R. Johnson, Ocean acidification reverses the positive effects of seawater pH fluctuations on growth and photosynthesis of the habitat-forming kelp, *Ecklonia radiata*, Sci. Rep. 6 (2016) 26036, doi:10.1038/srep26036.

[16] A.A. Briggs, R.C. Carpenter, Contrasting responses of photosynthesis and photochemical efficiency to ocean acidification under different light environments in a calcifying alga, Sci. Rep. 9 (2019) 3986, doi:10.1038/s41598-019-40620-8.

[17] R.P. Clark, M.S. Edwards, M.S. Foster, Effects of shade from multiple kelp canopies on an understory algal assemblage, Mar. Ecol. Prog. Ser. 267 (2004) 107–119, doi:10.3354/meps267107.

[18] O.W. Burnell, B.D. Russell, A.D. Irving, S.D. Connell, Seagrass response to CO_2 contingent on epiphytic algae–Indirect effects can overwhelm direct effects, Oecologia 176 (2014) 871–882, doi:10.1007/s00442-014-3054-z.

[19] J. Short, G.A. Kendrick, J. Falter, M.T. McCulloch, Interactions between filamentous turf algae and coralline algae are modified under ocean acidification, J. Exp. Mar. Biol. Ecol. 456 (2014) 70–77, doi:10.1016/j.jembe.2014.03.014.

[20] C.E. Cornwall, C.A. Pilditch, C.D. Hepburn, C.L. Hurd, Canopy macroalgae influence understorey corallines' metabolic control of near-surface pH and oxygen concentration, Mar. Ecol. Prog. Ser. 525 (2015) 81–95, doi:10.3354/meps11190.

[21] R.S. Steneck, M.H. Graham, B.J. Bourque, D. Corbett, J.M. Erlandson, J.A. Estes, M.J. Tegner, Kelp forest ecosystems–Biodiversity, stability, resilience and future, Environ. Conserv. 29 (2002) 436–459, doi:10.1017/S0376892902000322.

[22] N.T. Shears, R.C. Babcock, Quantitative Description of Mainland New Zealand's Shallow Subtidal Reef Communities, Science for Conservation 280, Department of Conservation, Wellington, 2007.

[23] A.N.C. Morse, D.E. Morse, Flypapers for coral and other planktonic larvae, Bioscience 46 (1996) 254–262, doi:10.2307/1312832.

[24] W.A. Nelson, Calcified macroalgae - critical to coastal ecosystems and vulnerable to change–A review, Mar. Freshw. Res. 60 (2009) 787–801, doi:10.1071/MF08335.

[25] H. Chenelot, S.C. Jewett, M.K. Hoberg, Macrobenthos of the nearshore Aleutian Archipelago, with emphasis on invertebrates associated with *Clathromorphum nereostratum* (Rhodophyta, Corallinaceae), Mar. Biodivers. 41 (2011) 413–424, doi:10.1007/s12526-010-0071-y.

[26] J. Tebben, C.A. Motti, N. Siboni, D.M. Tapiolas, A.P. Negri, P.J. Schupp, M. Kitamura, M. Hatta, P.D. Steinberg, T. Harder, Chemical mediation of coral larval settlement by crustose coralline algae, Sci. Rep. 5 (2015) 10803, doi:10.1038/srep10803.

[27] M.I. Bilan, A.I. Usov, Polysaccharides of calcareous algae and their effect on the calcification process, Russ. J. Bioorg. Chem. 27 (2001) 2–16, doi:10.1023/A:1009584516443.

[28] M.C. Nash, G. Diaz-Pulido, A.S. Harvey, W. Adey, Coralline algal calcification–A morphological and process-based understanding, PLoS One 14 (2019) e0221396, doi:10.1371/journal.pone.0221396.

[29] A.J. Andersson, F.T. Mackenzie, N.R. Bates, Life on the margin–Implications of ocean acidification on Mg-calcite, high latitude and cold-water marine calcifiers, Mar. Ecol. Prog. Ser. 373 (2008) 265–273, doi:10.3354/meps07639.

[30] J.B. Ries, Skeletal mineralogy in a high-CO_2 world, J. Exp. Mar. Biol. Ecol. 403 (2011) 54–64, doi:10.1016/j.jembe.2011.04.006.

[31] C.E. Cornwall, B.P. Harvey, S. Comeau, D.L. Cornwall, J.M. Hall-Spencer, V. Peña, S. Wada, L. Porzio, Understanding coralline algal responses to ocean acidification–Meta-analysis and synthesis, Glob. Change Biol. (2021) Advance online publication, doi:10.1111/gcb.15899.

[32] I.B. Kuffner, A.J. Andersson, P.L. Jokiel, K.S. Rodgers, F.T. Mackenzie, Decreased abundance of crustose coralline algae due to ocean acidification, Nat. Geosci. 1 (2008) 114–117, doi:10.1038/ngeo100.

[33] K.J. Kroeker, R.L. Kordas, R. Crim, I.E. Hendriks, L. Ramajo, G.S. Singh, C.M. Duarte, J.-.P. Gattuso, Impacts of ocean acidification on marine organisms–Quantifying sensitivities and interaction with warming, Glob. Change Biol. 19 (2013) 1884–1896, doi:10.1111/gcb.12179.

[34] L. Hofmann, K. Bischof, Ocean acidification effects on calcifying macroalgae, Aquat. Biol. 22 (2014) 261–279, doi:10.3354/ab00581.

[35] S.J. McCoy, N.A. Kamenos, Coralline algae (Rhodophyta) in a changing world–Integrating ecological, physiological, and geochemical responses to global change, J. Phycol. 51 (2015) 6–24, doi:10.1111/jpy.12262.

[36] C.D. Hepburn, D.W. Pritchard, C.E. Cornwall, R.J. McLeod, J. Beardall, J.A. Raven, C.L. Hurd, Diversity of carbon use strategies in a kelp forest community–Implications for a high CO_2 ocean, Glob. Change Biol. 17 (2011) 2488–2497, doi:10.1111/j.1365-2486.2011.02411.x.

[37] L.C. Hofmann, S. Straub, K. Bischof, Competition between calcifying and noncalcifying temperate marine macroalgae under elevated CO_2 levels, Mar. Ecol. Prog. Ser. 464 (2012) 89–105, doi:10.3354/meps09892.

[38] K.J. Kroeker, F. Micheli, M.C. Gambi, Ocean acidification causes ecosystem shifts via altered competitive interactions, Nat. Clim. Change 3 (2013) 156–159, doi:10.1038/nclimate1680.

[39] L.A. Gomez-Lemos, G. Diaz-Pulido, Crustose coralline algae and associated microbial biofilms deter seaweed settlement on coral reefs, Coral Reefs 36 (2017) 453–462, doi:10.1007/s00338-017-1549-x.

[40] L. Porzio, M.C. Buia, J.M. Hall-Spencer, Effects of ocean acidification on macroalgal communities, J. Exp. Mar. Biol. Ecol. 400 (2011) 278–287, doi:10.1016/j.jembe.2011.02.011.

[41] K.E. Fabricius, S.H.C. Noonan, D. Abrego, L. Harrington, G. De'ath, Low recruitment due to altered settlement substrata as primary constrain for coral communities under ocean acidification, Proc. R. Soc. B 284 (2017) 20171536 http://dx.doi.org/, doi:10.1098/rspb.2017.1536.

[42] C.E. Cornwall, S. Comeau, N.A. Kornder, C.T. Perry, R. van Hooidonk, T.M. DeCarlo, M.S. Pratchett, K.D. Anderson, N. Browne, R. Carpenter, G. Diaz-Pulido, J.P. D'Olivo, S.S. Doo, J. Figueiredo, S.A.V. Fortunato, E. Kennedy, C.A. Lantz, M.T. McCulloch, M. González-Rivero, V. Schoepf, S.G. Smithers, R.J. Lowe, Global declines in coral reef calcium carbonate production under ocean acidification and warming, Proc. Natl. Acad. Sci. 118 (2021) e2015265118, doi:10.1073/pnas.2015265118.

[43] A. Pentecost, Calcification and photosynthesis in *Corallina officinalis* L. using the $^{14}CO_2$ method, Br. Phycol. J. 13 (1978) 383–390, doi:10.1080/00071617800650431.

[44] D.D. Beer, A.W.D. Larkum, Photosynthesis and calcification in the calcifying algae *Halimeda discoidea* studied with microsensors, Plant Cell Environ. 24 (2001) 1209–1217, doi:10.1046/j.1365-3040.2001.00772.x.

[45] S. Teichert, A. Freiwald, Polar coralline algal $CaCO_3$-production rates correspond to intensity and duration of the solar radiation, Biogeoscience 11 (2014) 833–842, doi:10.5194/bg-11-833-2014.

[46] Z. Wei, C. Long, F. Yang, L. Long, Y. Huo, D. Ding, J. Mo, Increased irradiance availability mitigates the physiological performance of species of the calcifying green macroalga Halimeda in response to ocean acidification, Algal Res. 48 (2020) 101906, doi:10.1016/j.algal.2020.101906.

[47] K. Lüning, Seaweeds–Their Environment, Biogeography, and Ecophysiology, John Wiley & Sons, New York, 1990.

[48] R.D. Roberts, M. Kühl, R.N. Glud, S. Rysgaard, Primary production of crustose coralline red algae in a high Arctic fjord, J. Phycol. 38 (2002) 273–283, doi:10.1046/j.1529-8817.2002.01104.x.

[49] S. Martin, M.-.D. Castets, J. Clavier, Primary production, respiration and calcification of the temperate free-living coralline alga *Lithothamnion corallioides*, Aquat. Bot. 85 (2006) 121–128, doi:10.1016/j.aquabot.2006.02.005.

[50] J. Fietzke, F. Ragazzola, J. Halfar, H. Dietze, L.C. Foster, T.H. Hansteen, A. Eisenhauer, R.S. Steneck, Century-scale trends and seasonality in pH and temperature for shallow zones of the Bering Sea, Proc. Natl. Acad. Sci. 112 (2015) 2960–2965, doi:10.1073/pnas.1419216112.

[51] C.E. Cornwall, S. Comeau, M.T. McCulloch, Coralline algae elevate pH at the site of calcification under ocean acidification, Glob. Change Biol. 23 (2017) 4245–4256, doi:10.1111/gcb.13673.

[52] C. McNicholl, M.S. Koch, L.C. Hofmann, Photosynthesis and light-dependent proton pumps increase boundary layer pH in tropical macroalgae–A proposed mechanism to sustain calcification under ocean acidification, J. Exp. Mar. Biol. Ecol. 521 (2019) 151208, doi:10.1016/j.jembe.2019.151208.

[53] A. Freiwald, R. Henrich, Reefal coralline algal build-ups within the Arctic Circle–Morphology and sedimentary dynamics under extreme environmental seasonality, Sedimentology 41 (1994) 963–984, doi:10.1111/j.1365-3091.1994.tb01435.x.

[54] L.C. Hofmann, K. Schoenrock, D. de Beer, Arctic coralline algae elevate surface pH and carbonate in the dark, Front. Plant Sci. 9 (2018) 1496, doi:10.3389/fpls.2018.01416.

[55] A.K. Barner, F. Chan, A. Hettinger, S.D. Hacker, K. Marshall, B.A. Menge, Generality in multispecies responses to ocean acidification revealed through multiple hypothesis testing, Glob. Change Biol. 24 (2018) 4464–4477, doi:10.1111/gcb.14372.

[56] B. Gaylord, J.H. Rosman, D.C. Reed, J.R. Koseff, J. Fram, S. MacIntyre, K. Arkema, C. McDonald, M.A. Brzezinski, J.L. Largier, S.G. Monismith, P.T. Raimondi, B. Mardian, Spatial patterns of flow and their modification within and around a giant kelp forest, Limnol. Oceanogr. 52 (2007) 1838–1852, doi:10.4319/lo.2007.52.5.1838.

[57] J.A. Short, O. Pedersen, G.A. Kendrick, Turf algal epiphytes metabolically induce local pH increase, with implications for underlying coralline algae under ocean acidification, Estuar. Coast. Shelf Sci. 164 (2015) 463–470, doi:10.1016/j.ecss.2015.08.006.

[58] F. Noisette, C. Hurd, Abiotic and biotic interactions in the diffusive boundary layer of kelp blades create a potential refuge from ocean acidification, Funct. Ecol. 32 (2018) 1329–1342, doi:10.1111/1365-2435.13067.

[59] D.A. Koweek, K.J. Nickols, P.R. Leary, S.Y. Litvin, T.W. Bell, T. Luthin, S. Lummis, D.A. Mucciarone, R.B. Dunbar, A year in the life of a central California kelp forest–Physical and biological insights into biogeochemical variability, Biogeoscience 14 (2017) 31–44, doi:10.5194/bg-14-31-2017.

[60] H.K. Hirsh, K.J. Nickols, Y. Takeshita, S.B. Traiger, D.A. Mucciarone, S. Monismith, R.B. Dunbar, Drivers of biogeochemical variability in a central California kelp forest–Implications for local amelioration of ocean acidification, J. Geophys. Res. Oceans 125 (2020) e2020JC016320, doi:10.1029/2020JC016320.

[61] C.E. Cornwall, C.D. Hepburn, C.A. Pilditch, C.L. Hurd, Concentration boundary layers around complex assemblages of macroalgae–Implications for the effects of ocean acidification on understory coralline algae, Limnol. Oceanogr. 58 (2013) 121–130, doi:10.4319/lo.2013.58.1.0121.

[62] C.E. Cornwall, P.W. Boyd, C.M. McGraw, C.D. Hepburn, C.A. Pilditch, J.N. Morris, A.M. Smith, C.L. Hurd, Diffusion boundary layers ameliorate the negative effects of ocean acidification on the temperate coralline macroalga *Arthrocardia corymbosa*, PLoS One 9 (2014) e97235, doi:10.1371/journal.pone.0097235.

[63] C.L. Hurd, Slow-flow habitats as refugia for coastal calcifiers from ocean acidification, J. Phycol. 51 (2015) 599–605, doi:10.1111/jpy.12307.

[64] D. Krause-Jensen, N. Marbà, M. Sanz-Martin, I.E. Hendriks, J. Thyrring, J. Carstensen, M.K. Sejr, C.M. Duarte, Long photoperiods sustain high pH in Arctic kelp forests, Sci. Adv. 2 (2016) e1501938, doi:10.1126/sciadv.1501938.

[65] T. Guy-Haim, J. Silverman, M. Wahl, J. Aguirre, F. Noisette, G. Rilov, Epiphytes provide microscale refuge from ocean acidification, Mar. Environ. Res. 161 (2020) 105093, doi:10.1016/j.marenvres.2020.105093.

[66] S. Comeau, C.E. Cornwall, C.A. Pupier, T.M. DeCarlo, C. Alessi, R. Trehern, M.T. McCulloch, Flow-driven micro-scale pH variability affects the physiology of corals and coralline algae under ocean acidification, Sci. Rep. 9 (2019) 12829, doi:10.1038/s41598-019-49044-w.

[67] C.E. Cornwall, C.D. Hepburn, C.M. McGraw, K.I. Currie, C.A. Pilditch, K.A. Hunter, P.W. Boyd, C.L. Hurd, Diurnal fluctuations in seawater pH influence the response of a calcifying macroalga to ocean acidification, Proc. R. Soc. B Biol. Sci. 280 (2013) 20132201, doi:10.1098/rspb.2013.2201.

[68] M.Y. Roleda, C.E. Cornwall, Y. Feng, C.M. McGraw, A.M. Smith, C.L. Hurd, Effect of ocean acidification and pH fluctuations on the growth and development of coralline algal recruits, and an associated benthic algal assemblage, PLoS One 10 (2015) e0140394, doi:10.1371/journal.pone.0140394.

[69] M.D. Johnson, L.M. Rodriguez Bravo, S.E. O'Connor, N.F. Varley, A.H. Altieri, pH variability exacerbates effects of ocean acidification on a Caribbean crustose coralline alga, Front. Mar. Sci. 6 (2019) 150, doi:10.3389/fmars.2019.00150.

[70] F. Bulleri, Duration of overgrowth affects survival of encrusting coralline algae, Mar. Ecol. Prog. Ser. 321 (2006) 79–85, doi:10.3354/meps321079.

[71] D.R. Schiel, M.S. Foster, The Biology and Ecology of Giant Kelp Forests, Univ of California Press, Oakland, 2015.

[72] W. Evans, J.T. Mathis, J. Ramsay, J. Hetrick, On the frontline–Tracking ocean acidification in an Alaskan shellfish hatchery, PLoS One 10 (2015) e0130384, doi:10.1371/journal.pone.0130384.

[73] R.A. Feely, C.L. Sabine, K. Lee, W. Berelson, J. Kleypas, V.J. Fabry, F.J. Millero, Impact of anthropogenic CO_2 on the $CaCO_3$ system in the oceans, Science 305 (2004) 362–366, doi:10.1126/science.1097329.

[74] M. Steinacher, F. Joos, T.L. Frolicher, G.-.K. Plattner, S.C. Doney, Imminent ocean acidification in the Arctic projected with the NCAR global coupled carbon cycle-climate model, Biogeoscience 6 (2009) 515–533, doi:10.5194/bg-6-515-2009.

[75] V.J. Fabry, J.B. McClintock, J.T. Mathis, J.M. Grebmeier, Ocean acidification at high latitudes–The bellweather, Oceanography 22 (2009) 160–171 http://www.jstor.org/stable/24861032.

[76] B.A. Twist, K.F. Neill, J. Bilewitch, S.Y. Jeong, J.E. Sutherland, W.A. Nelson, High diversity of coralline algae in New Zealand revealed–Knowledge gaps and implications for future research, PLoS One 14 (2019) e0225645, doi:10.1371/journal.pone.0225645.

[77] B. Twist, C. Cornwall, S. McCoy, P. Gabrielson, P. Martone, W. Nelson, The need to employ reliable and reproducible species identifications in coralline algal research, Mar. Ecol. Prog. Ser. 654 (2020) 225–231, doi:10.3354/meps13506.

[78] B. Gaylord, K.J. Kroeker, J.M. Sunday, K.M. Anderson, J.P. Barry, N.E. Brown, S.D. Connell, S. Dupont, K.E. Fabricius, J.M. Hall-Spencer, T. Klinger, M. Milazzo, P.L. Munday, B.D. Russell, E. Sanford, S.J. Schreiber, V. Thiyagarajan, M.L.H. Vaughan, S. Widdicombe, C.D.G. Harley, Ocean acidification through the lens of ecological theory, Ecology 96 (2015) 3–15, doi:10.1890/14-0802.1.

[79] K.J. Kroeker, R.L. Kordas, C.D.G. Harley, Embracing interactions in ocean acidification research–Confronting multiple stressor scenarios and context dependence, Biol. Lett. 13 (2017) 20160802, doi:10.1098/rsbl.2016.0802.

[80] J.R. Hughey, P.C. Silva, M.H. Hommersand, Solving taxonomic and nomenclatural problems in Pacific Gigartinaceae (Rhodophyta) using DNA from type material, J. Phycol. 37 (2001) 1091–1109, doi:10.1046/j.1529-8817.2001.01048.x.

[81] P.W. Gabrielson, K.A. Miller, P.T. Martone, Morphometric and molecular analyses confirm two distinct species of *Calliarthron* (Corallinales, Rhodophyta), a genus endemic to the northeast Pacific, Phycologia 50 (2011) 298–316, doi:10.2216/10-42.1.

[82] D.W. Freshwater, J. Rueness, Phylogenetic relationships of some European Gelidium (Gelidiales, Rhodophyta) species, based on *rbcL* nucleotide sequence analysis, Phycologia 33 (1994) 187–194, doi:10.2216/i0031-8884-33-3-187.1.

[83] B. Thiers, Index Herbariorum–A Global Directory of Public Herbaria and Associated Staff, Botanical Garden Virtual Herbarium, New York, 2021 http://sweetgum.nybg.org/ih/ (accessed May 25, 2021).
[84] B. Lewis, G. Diaz-Pulido, Suitability of three fluorochrome markers for obtaining in situ growth rates of coralline algae, J. Exp. Mar. Biol. Ecol. 490 (2017) 64–73, doi:10.1016/j.jembe.2017.02.004.
[85] R Core TeamR–A Language and Environment for Statistical Computing, R Foundation for Statistical Computing, Vienna, Austria, 2021 https://www.R-project.org/.
[86] J.T. Mathis, S.R. Cooley, N. Lucey, S. Colt, J. Ekstrom, T. Hurst, C. Hauri, W. Evans, J.N. Cross, R.A. Feely, Ocean acidification risk assessment for Alaska's fishery sector, Prog. Oceanogr. 136 (2015) 71–91, doi:10.1016/j.pocean.2014.07.001.
[87] A.G. Dickson, C.L. Sabine, J.R. Christian, in: Guide to Best Practices for Ocean CO_2 Measurements, 3, PICES Special Publication, 2007, pp. 1–191. http://dx.doi.org/10.25607/OBP-1342.
[88] C. Mehrbach, C.H. Culberson, J.E. Hawley, R.M. Pytkowicx, Measurement of the apparent dissociation constants of carbonic acid in seawater at atmospheric pressure, Limnol. Oceanogr. 18 (1973) 897–907, doi:10.4319/lo.1973.18.6.0897.
[89] A.G. Dickson, F.J. Millero, A comparison of the equilibrium constants for the dissociation of carbonic acid in seawater media, Deep-Sea Res. 34 (1987) 1733–1743, doi:10.1016/0198-0149(87)90021-5.
[90] E.R. Lewis, D.W.R. Wallace, Program developed for CO2 system calculations, ORNL/CDIAC-105, Carbon Dioxide Inf. Anal. Cent., Oak Ridge Natl. Lab, Oak Ridge, Tenn., 1998, 38 pp. 10.15485/1464255
[91] P.L. Jokiel, J.E. Maragos, L. Franzisket, Coral growth–Buoyant weight technique, in: D.R. Stoddart, R.E. Johannes (Eds.), Coral Reefs–Research Methods, UNESCO, Paris, 1978, pp. 529–542.
[92] S.V. Smith, G.S. Key, Carbon dioxide and metabolism in marine environments, Limnol. Oceanogr. 20 (1975) 493–495, doi:10.4319/lo.1975.20.3.0493.
[93] T. Platt, C.L. Gallegos, W.G. Harrison, Photoinhibition of photosynthesis in natural assemblages of marine phytoplankton, J. Mar. Res. (1980) 687–701.
[94] C.E. Cornwall, S. Comeau, T.M. DeCarlo, E. Larcombe, B. Moore, K. Giltrow, F. Puerzer, Q. D'Alexis, M.T. McCulloch, A coralline alga gains tolerance to ocean acidification over multiple generations of exposure, Nat. Clim. Change 10 (2020) 143–146, doi:10.1038/s41558-019-0681-8.
[95] B. Moore, S. Comeau, M. Bekaert, A. Cossais, A. Purdy, E. Larcombe, F. Puerzer, M.T. McCulloch, C.E. Cornwall, Rapid multi-generational acclimation of coralline algal reproductive structures to ocean acidification, Proc. R. Soc. B 288 (2021) 20210130, doi:10.1098/rspb.2021.0130.
[96] J.E. Kübler, A.M. Johnston, J.A. Raven, The effects of reduced and elevated CO_2 and O_2 on the seaweed *Lomentaria articulata,* Plant Cell Environ. 22 (1999) 1303–1310, doi:10.1046/j.1365-3040.1999.00492.x.
[97] S.J. McCoy, Morphology of the crustose coralline alga *Pseudolithophyllum muricatum* (Corallinales, Rhodophyta) responds to 30 years of ocean acidification in the Northeast Pacific, J. Phycol. 49 (2013) 830–837, doi:10.1111/jpy.12095.
[98] F. Ragazzola, L.C. Foster, A.U. Form, J. Büscher, T.H. Hansteen, J. Fietzke, Phenotypic plasticity of coralline algae in a high CO_2 world, Ecol. Evol. 3 (2013) 3436–3446, doi:10.1002/ece3.723.
[99] F. Ragazzola, L.C. Foster, C.J. Jones, T.B. Scott, J. Fietzke, M.R. Kilburn, D.N. Schmidt, Impact of high CO_2 on the geochemistry of the coralline algae *Lithothamnion glaciale*, Sci. Rep. 6 (2016) 20572, doi:10.1038/srep20572.
[100] S.J. McCoy, F. Ragazzola, Skeletal trade-offs in coralline algae in response to ocean acidification, Nat. Clim. Change 4 (2014) 719–723, doi:10.1038/nclimate2273.
[101] L. Kwiatkowski, B. Gaylord, T. Hill, J. Hosfelt, K.J. Kroeker, Y. Nebuchina, A. Ninokawa, A.D. Russell, E.B. Rivest, M. Sesboüé, K. Caldeira, Nighttime dissolution in a temperate coastal ocean ecosystem increases under acidification, Sci. Rep. 6 (2016) 22984, doi:10.1038/srep22984.
[102] E. Bergstrom, A. Ordoñez, M. Ho, C. Hurd, B. Fry, G. Diaz-Pulido, Inorganic carbon uptake strategies in coralline algae–Plasticity across evolutionary lineages under ocean acidification and warming, Mar. Environ. Res. 161 (2020) 105107, doi:10.1016/j.marenvres.2020.105107.
[103] S. Comeau, R.C. Carpenter, P.J. Edmunds, Coral reef calcifiers buffer their response to ocean acidification using both bicarbonate and carbonate, Proc. R. Soc. B Biol. Sci. 280 (2013) 20122374, doi:10.1098/rspb.2012.2374.
[104] L.C. Hofmann, S. Heesch, Latitudinal trends in stable isotope signatures and carbon-concentrating mechanisms of northeast Atlantic rhodoliths, Biogeoscience 15 (2018) 6139–6149, doi:10.5194/bg-15-6139-2018.
[105] S. Comeau, R.C. Carpenter, P.J. Edmunds, Effects of irradiance on the response of the coral *Acropora pulchra* and the calcifying alga *Hydrolithon reinboldii* to temperature elevation and ocean acidification, J. Exp. Mar. Biol. Ecol. 453 (2014) 28–35, doi:10.1016/j.jembe.2013.12.013.
[106] C.D.G. Harley, K.M. Anderson, K.W. Demes, J.P. Jorve, R.L. Kordas, T.A. Coyle, M.H. Graham, Effects of climate change on global seaweed communities, J. Phycol. 48 (2012) 1064–1078, doi:10.1111/j.1529-8817.2012.01224.x.
[107] A. Kumar, H. AbdElgawad, I. Castellano, S. Selim, G.T.S. Beemster, H. Asard, M.C. Buia, A. Palumbo, Effects of ocean acidification on the levels of primary and secondary metabolites in the brown macroalga *Sargassum vulgare* at different time scales, Sci. Total Environ. 643 (2018) 946–956, doi:10.1016/j.scitotenv.2018.06.176.
[108] A. Kumar, M.C. Buia, A. Palumbo, M. Mohany, M.A.M. Wadaan, W.N. Hozzein, G.T.S. Beemster, H. AbdElgawad, Ocean acidification affects biological activities of seaweeds–A case study of *Sargassum vulgare* from Ischia volcanic CO_2 vents, Environ. Pollut. 259 (2020) 113765, doi:10.1016/j.envpol.2019.113765.
[109] D.C. Reed, M.S. Foster, The effects of canopy shadings on algal recruitment and growth in a giant kelp forest, Ecology 65 (1984) 937–948, doi:10.2307/1938066.
[110] J.-.P. Gattuso, A. Magnan, R. Billé, W.W.L. Cheung, E.L. Howes, F. Joos, D. Allemand, L. Bopp, S.R. Cooley, C.M. Eakin, O. Hoegh-Guldberg, R.P. Kelly, H.-.O. Pörtner, A.D. Rogers, J.M. Baxter, D. Laffoley, D. Osborn, A. Rankovic, J. Rochette, U.R. Sumaila, S. Treyer, C. Turley, Contrasting futures for ocean and society from different anthropogenic CO_2 emissions scenarios, Science 349 (2015) aac4722 http://dx.doi.org/, doi:10.1126/science.aac4722.
[111] C.E. Cornwall, G. Diaz-Pulido, S. Comeau, Impacts of ocean warming on coralline algal calcification–Meta-analysis, knowledge gaps, and key recommendations for future research, Front. Mar. Sci. 6 (2019) 186, doi:10.3389/fmars.2019.00186.
[112] R.M. Vásquez-Elizondo, S. Enríquez, Coralline algal physiology is more adversely affected by elevated temperature than reduced pH, Sci. Rep. 6 (2016) 19030, doi:10.1038/srep19030.
[113] S. Martin, J.-.P. Gattuso, Response of Mediterranean coralline algae to ocean acidification and elevated temperature, Glob. Change Biol. 15 (2009) 2089–2100, doi:10.1111/j.1365-2486.2009.01874.x.
[114] F. Noisette, H. Egilsdottir, D. Davoult, S. Martin, Physiological responses of three temperate coralline algae from contrasting habitats to near-future ocean acidification, J. Exp. Mar. Biol. Ecol. 448 (2013) 179–187, doi:10.1016/j.jembe.2013.07.006.
[115] F. Ragazzola, L.C. Foster, A. Form, P.S.L. Anderson, T.H. Hansteen, J. Fietzke, Ocean acidification weakens the structural integrity of coralline algae, Glob. Change Biol. 18 (2012) 2804–2812, doi:10.1111/j.1365-2486.2012.02756.x.
[116] S.J. McCoy, C.A. Pfister, Historical comparisons reveal altered competitive interactions in a guild of crustose coralline algae, Ecol. Lett. 17 (2014) 475–483, doi:10.1111/ele.12247.
[117] K.M. Schoenrock, J.B. Schram, C.D. Amsler, J.B. McClintock, R.A. Angus, Y.K. Vohra, Climate change confers a potential advantage to fleshy Antarctic crustose macroalgae over calcified species, J. Exp. Mar. Biol. Ecol. 474 (2016) 58–66, doi:10.1016/j.jembe.2015.09.009.